Transcriptome differences between Cupriavidus necator NH9 grown with 3-chlorobenzoate and that grown with benzoate

Transcriptome differences between *Cupriavidus necator* NH9 grown with 3-chlorobenzoate and that grown with benzoate

A short running head: RNA-seq of 3-chlorobenzoate degradative bacterium

Ryota Moriuchi[1,2], Hideo Dohra[1], Yu Kanesaki[1] and Naoto Ogawa[2,3*]

[1]Research Institute of Green Science and Technology, Shizuoka University, 836 Ohya, Suruga-ku, Shizuoka-shi, Shizuoka 422-8529, Japan

[2]The United Graduate School of Agricultural Science, Gifu University, 1-1 Yanagido, Gifu-shi, Gifu 501-1193, Japan

[3]Graduate School of Integrated Science and Technology, Shizuoka University, 836 Ohya, Suruga-ku, Shizuoka-shi, Shizuoka 422-8529, Japan

*Address correspondence to Naoto Ogawa, Faculty of Agriculture, Shizuoka University, 836 Ohya, Suruga-ku, Shizuoka-shi, Shizuoka, 422-8529, Japan. Tel/Fax: +81-54-238-4875 / +81-54-237-3028; e-mail: ogawa.naoto@shizuoka.ac.jp

Abstract

RNA-seq analysis of *Cupriavidus necator* NH9, a 3-chlorobenzoate degradative bacterium, cultured with 3-chlorobenzaote and benzoate, revealed strong induction of genes encoding enzymes in degradation pathways of the respective compound, including the genes to convert 3-chlorobenzaote and benzoate to chlorocatechol and catechol, respectively, and the genes of chlorocatechol *ortho*-cleavage pathway for conversion to central metabolites. The genes encoding transporters, components of the stress response, flagellar proteins, and chemotaxis proteins showed altered expression patterns between 3-chlorobenzoate and benzoate. Gene Ontology enrichment analysis revealed that chemotaxis related terms were significantly upregulated by benzoate compared with 3-chlorobenzoate. Consistent with this, in semi-solid agar plate assays, NH9 cells showed stronger chemotaxis to benzoate than to 3-chlorobenzoate. These results, combined with the absence of genes related to uptake/chemotaxis for 3-chlorobenzoate located closely to the degradation genes of 3-chlorobenzoate, suggested that NH9 has not fully adapted to the utilization of chlorinated benzoate, unlike benzoate, in nature.

Keywords: 3-chlorobenzoate; benzoate; chemotaxis; *Cupriavidus*; RNA-seq

31 Aromatic compounds are one of the most widely distributed classes of organic compounds
32 in nature. These compounds include aromatic amino acids, flavonoids, lignin components,
33 and constituents of fossil fuels or compounds derived from human activities (e.g.,
34 solvents, agrochemicals, and polychlorinated biphenyls: PCBs, etc.). They are generally
35 recalcitrant and persistent in the environment. Some of them are toxic to ecosystems or
36 may be converted to hazardous products via natural processes. Therefore, these
37 compounds should be removed promptly from the environment. Bioremediation is a
38 process that utilizes the metabolic versatility of living organisms, mostly microorganisms
39 and plants, to degrade or detoxify pollutants. Some microorganisms in soils and water can
40 convert these organic chemicals to inorganic products (Alexander 1981; Reineke 1998;
41 van der Meer *et al*. 1992). To develop a useful strategy for the bioremediation of aromatic
42 compounds, it is important to understand microbial behavior in response to such aromatic
43 compounds and the molecular mechanisms underlying their decomposition by
44 microorganisms.

45 Transcriptome analysis is an effective method to observe gene expression under
46 different environmental conditions. Genome-wide expression profiling by DNA
47 microarray analyses or next-generation sequencing techniques has been used to study
48 many aromatic compound-degrading bacteria, including *Bacillus subtilis* NCIB 3610
49 (hydroxylated PCBs, methoxylated PCBs, and PCBs) (Sun *et al*. 2018), *Bradyrhizobium*
50 *japonicum* USDA110 (4-hydroxybenzoate: 4-HBA, protocatechuate, vanillate, and
51 vanillin) (Ito *et al*. 2006), *Comamonas testosteroni* WDL7 (3-chloroaniline) (Wu *et al*.
52 2016), *Cupriavidus pinatubonensis* JMP134 (2,4-dichlorophenoxyacetic acid: 2,4-D)
53 (Dennis *et al*. 2003), *Mycobacterium* sp. A1-PYR (phenanthrene and pyrene) (Yuan *et al*.
54 2018), *Novosphingobium* sp. LH128 (phenanthrene) (Fida *et al*. 2017), *Paraburkholderia*

55 *xenovorans* LB400 (benzoate: BA, biphenyl, PCBs, and phenylacetate) (Denef *et al*. 2004,
56 2006; Parnell *et al*. 2006; Patrauchan *et al*. 2011), *Pseudomonas putida* (3-chlorobenzoate:
57 3-CB and carbazole) (Miyakoshi *et al*. 2007; Miyazaki *et al*. 2018; Wang *et al*. 2011),
58 *Rhodococcus aetherivorans* I24 (biphenyl and PCBs) (Puglisi *et al*. 2010), *Rhodococcus*
59 *jostii* RHA1 (BA, biphenyl, ethylbenzene, phthalate, and terephthalate) (Gonçalves *et al*.
60 2006; Hara *et al*. 2007; Iino *et al*. 2012), *Sinorhizobium meliloti* 1021 (indole-3-acetic
61 acid) (Imperlini *et al*. 2009), and *Sphingobium chlorophenolicum* L-1 (carbonyl cyanide
62 *m*-chlorophenyl hydrazone, paraquat, pentachlorophenol, and toluene) (Flood and Copley
63 2018). Their results revealed differentially expressed genes (DEGs) involved in the
64 degradation of aromatic compounds, stress responses, substrate transport, and
65 transcriptional regulatory function. However, to our knowledge, no previous studies have
66 tried to detect DEGs between a bacterium cultured with a simple chlorinated aromatic
67 compound and its analogous aromatic compound without chlorine. Identification of the
68 genes induced by chlorinated aromatic compounds will shed light on how microbes
69 perceive, respond to, and detoxify such substances.

70 Many members of the genus *Cupriavidus* in the family *Burkholderiaceae* are able
71 to degrade aromatic pollutants (Fang *et al*. 2019; Pérez-Pantoja *et al*. 2015; Xiang *et al*.
72 2020). For example, *Cupriavidus necator* strain NH9, isolated from a soil sample in Japan,
73 can utilize 3-CB as carbon and energy source (Ogawa and Miyashita 1995). In our
74 previous study, we sequenced the genome of NH9 and identified genes involved in
75 degradation pathways for aromatic compounds (including BA, catechol, and mono-
76 hydroxylated benzoates) shared by several strains of the genus *Cupriavidus* (Moriuchi *et*
77 *al*. 2019). Among the dozens of completely sequenced strains of *Cupriavidus*, strains NH9
78 (Moriuchi *et al*. 2019; Ogawa and Miyashita 1995), *Cupriavidus nantongensis* X1 (Fang

79 *et al*. 2019), *Cupriavidus oxalaticus* X32 (Xiang *et al*. 2020), and *C. pinatubonensis*
80 JMP134 (Pérez-Pantoja *et al*. 2015) have been reported to degrade chlorinated aromatic
81 compounds. Also, in these strains, transcriptome analysis was performed only in strain
82 JMP134 using 2,4-D, which focused on the expression of 2,4-D-degrading genes within
83 mixed microbial communities (Dennis *et al*. 2003). There has been no report of analysis of
84 whole transcriptome of *Cupriavidus* strains grown with chlorinated aromatic compound.
85 This prompted us to investigate the differences in genome wide gene expression in NH9,
86 whose transcriptional regulation of the degradative genes for chlorocatechol has been
87 characterized (Ogawa *et al*. 1999), between cells grown with 3-CB and those grown with
88 its non-chlorinated counterpart, BA. In studies on microbial degradation, chlorobenzoates
89 and BA have been used as model compounds for chlorinated and non-chlorinated
90 aromatics, respectively, because of their simple structures (Bott and Kaplan 2002; Gibson
91 and Harwood 2002). The results of this study reveal the differential gene expression
92 profiles of strain NH9 between cells grown with 3-CB and those grown with BA. Our
93 results imply that strain NH9 in the genus *Cupriavidus*, which is known to contain
94 biodegrading strains, has not fully adapted to utilize chlorinated aromatic compounds,
95 unlike natural aromatic compounds, in the environment.

96 **Materials and Methods**

97 *Bacterial strain, culture media, and growth experiment*

98 *C. necator* stain NH9 was grown on basal salts medium (BSM) (Ogawa and Miyashita
99 1995) supplemented with 5 mM 3-CB, BA, or citric acid (CA) at 30°C. All the chemical
100 reagents for media were purchased from Fujifilm-Wako (Osaka, Japan). Strain NH9 from
101 glycerol stock was inoculated onto BSM agar medium containing the respective carbon
102 source and incubated for 2 days. Subsequently, the cells were precultured in liquid

103 medium containing the respective carbon source with shaking at 120 rpm for 24 h. Then, a
104 portion of each preculture was inoculated into fresh culture medium containing the
105 corresponding carbon source. The amount of the volume of the preculture to be inoculated
106 to the fresh medium was adjusted so that the optical density at 600 nm (OD_{600}) of the
107 successive culture was 0.01 at the starting point. Also, the volume of the successive
108 culture was adjusted to 100 ml. For the growth experiment, cultures were shaken at 120
109 rpm and the OD_{600} was monitored using an Ultrospec 3000 spectrophotometer (Amersham
110 Pharmacia Biotech, Piscataway, NJ, USA).

111 *High performance liquid chromatography (HPLC) analysis to quantify aromatic*
112 *compounds*

113 For the HPLC analysis, 300 µl NH9 cell culture was collected and 100 µl methanol was
114 added to stop bacterial growth. The mixture was vortexed and then centrifuged at 9,100 ×
115 *g* for 3 min at 4°C. The supernatant was filtered through a 0.2-µm pore-size hydrophilic
116 PTFE membrane filter (Merck Millipore, Burlington, MA, USA) and then subjected to
117 HPLC analysis using a SCL-10A VP system (Shimadzu, Kyoto, Japan) equipped with a
118 YMC-Triart C18 column (150 mm × 4.6 mm, 5 µm; YMC, Kyoto, Japan). Water-
119 acetonitrile-acetic acid was used as the mobile phase for analysis of 3-CB (45:50:5, v/v)
120 and BA (75:20:5, v/v). The flow rate was 1 ml min^{-1} and the column temperature was held
121 constant at 37°C. A SPD-10AVi wavelength detector (Shimadzu) was used to detect 3-CB
122 at 200 nm and BA at 254 nm. The concentrations of aromatic compounds were calculated
123 from calibration curves.

124 *Total RNA extraction, cDNA library preparation, and RNA-sequencing*

125 The NH9 cells from three biologically independent cultures with each of the three carbon
126 sources were harvested at mid-growth phase (OD_{600} = 0.2 to 0.5). The cells were collected
127 by centrifugation (10,000 × *g* for 5 min at 4°C) and immediately treated with RNAprotect
128 Cell Reagent (QIAGEN, Hilden, Germany). The cells were collected by centrifugation
129 (8,000 × *g* for 10 min at room temperature) and then stored at −80°C until RNA isolation.
130 Total RNA was extracted using the RNeasy Mini Kit (QIAGEN), and contaminating DNA
131 was removed by two treatments with the Turbo DNA-free Kit (Thermo Fisher Scientific,
132 Waltham, MA, USA) following the manufacturer's instructions. The genomic DNA-
133 depleted RNA was further purified using the RNeasy Mini Kit following the
134 supplementary protocol. The quantity of the purified total RNA was measured by
135 fluorometry using the Qubit RNA HS Assay Kit (Thermo Fisher Scientific), and the
136 quality of the purified total RNA was assessed using an Agilent 2100 Bioanalyzer (Agilent
137 Technologies, Santa Clara, CA, USA), and TECAN Infinite M200 (TECAN, Mannedorf,
138 Switzerland) or Varioskan LUX (Thermo Fisher Scientific) plate readers. Ribosomal RNA
139 was removed from 5 μg purified total RNA using the Ribo-Zero rRNA Removal Kit for
140 Gram-negative bacteria (Illumina, San Diego, CA, USA), and the resultant mRNA was
141 purified using the RNeasy MinElute Cleanup Kit (QIAGEN) for cDNA synthesis.
142 Subsequently, cDNA libraries were prepared with 50 ng mRNA using the KAPA Stranded
143 mRNA-Seq Kit (Kapa Biosystems, Woburn, MA, USA) according to the manufacturer's
144 instructions, including the skipping mRNA capture protocol. The indexed cDNA libraries
145 were pooled and sequenced on a MiSeq system (Illumina) with 76-bp paired-end reads at
146 the Instrumental Research Support office, Research Institute of Green Science and
147 Technology, Shizuoka University, Japan. See Table S1 for detailed information about
148 RNA-seq read data.

149 *Mapping, read counts, and differential expression analysis*

150 The obtained raw reads were filtered with Trimmomatic version 0.36 (Bolger *et al*. 2014).
151 Adapter sequences, the terminal 76 bases, low-quality reads of < Q15, and reads of < 50
152 bp were trimmed. The cleaned reads were mapped to the NH9 complete genome sequence
153 (accession no. P017757 to CP017760) using HISAT2 version 2.1.0 (Kim *et al*. 2015) with
154 report alignments option (--dta) and strand-specific option (--rna-strandness RF). The
155 number of aligned reads was counted and transcripts per million (TPM) values were
156 calculated using StringTie version 1.3.5 (Pertea *et al*. 2015) with strand option (--rf). Read
157 counts data for differential expression inputs were generated using the prepDE.py script
158 (http://ccb.jhu.edu/software/stringtie/dl/prepDE.py). The DEGs were identified using
159 edgeR package version 3.24.3 (Robinson *et al*. 2010).

160 *Gene Ontology (GO) enrichment analysis*

161 All proteins were annotated by hmmscan (http://hmmer.org/) against the Pfam database
162 release 32.0 (Mitchell *et al*. 2015). The Pfam IDs were converted into GO terms using the
163 pfam2go conversion table
164 (http://current.geneontology.org/ontology/external2go/pfam2go) (Ashburner *et al*. 2000).
165 The parametric analysis of gene set enrichment (PAGE) method (Kim and Volsky 2005)
166 was used to detect a large number of significantly altered gene sets and functions. GO
167 terms with false discovery rate (FDR) < 0.05 were considered statistically significant.

168 *Semi-solid agar plate assays*

169 The chemotactic behavior of strain NH9 towards aromatic compounds was tested in semi-
170 solid agar plate assays (Yamamoto-Tamura *et al*. 2015). For these assays, 100 ml NH9
171 cell culture in the early stationary phase ($O.D._{600}$ ~0.8) was centrifuged (1,600 × *g* for 5

172 min at 4°C), then the pelleted cells were washed twice with BSM and resuspended in 25
173 ml BSM containing 0.2% (w/v) agar. Aliquots (5 ml) of resuspended cells were poured
174 into 60-mm-diameter plastic Petri plates. Then, an 8-mm-diameter filter paper disk that
175 was spotted with 20 µl 500 mM 3-CB or BA, or a 5% (w/v) solution of casamino acids
176 (positive control), was placed in the center of each Petri plate. In the negative control,
177 filter paper was spotted with 20 µl BSM without any carbon source. The chemotactic
178 response was observed after 3 to 14 h of incubation at 25°C.

179 **Results**

180 ***Growth of NH9 and its ability to degrade aromatic compounds***

181 *C. necator* strain NH9 was grown on BSM containing 5 mM 3-CB, BA, or CA. Strain
182 NH9 was able to grow well with all three compounds although the growth rate was
183 slightly lower with 3-CB than with BA and CA (Fig. 1A). HPLC analyses confirmed that
184 both 3-CB and BA were completely degraded within 18 h of culture with NH9 (Fig. 1B).
185 Compared with BA, 3-CB showed a slight time lag before degradation. Even after these
186 compounds were decomposed thoroughly, the OD_{600} did not decrease quickly.

187 ***Analysis of differentially expressed genes***

188 To identify commonly and specifically expressed genes between NH9 cells cultured with
189 3-CB and those cultured with BA, we conducted transcriptome analyses. Reverse-
190 transcribed ribosomal-RNA depleted RNA samples were sequenced on the Illumina
191 MiSeq platform (Illumina) (Table S1). Prior to differential expression analysis, we
192 evaluated similarities and variations in overall gene expression datasets among the
193 samples. The biological replicates clustered closely in multi-dimensional scaling (MDS)
194 plot and cluster dendrogram analyses (Fig. S1), indicative of very little variation among

195 replicates. Genes that met the criteria of log fold-change (logFC) ≥ 2 or ≤ -2 with FDR <
196 0.05 were considered to be significantly differentially expressed between compared pairs
197 of samples. First we compared the transcriptome of NH9 between cells grown with 3-CB
198 and cells grown with BA. In total, 263 genes were expressed differentially: 137 genes
199 were upregulated and 126 genes were downregulated in the 3-CB sample compared with
200 the BA sample. In the 3-CB sample compared with the CA sample, 591 genes were
201 expressed differentially: 374 were upregulated and 217 were downregulated. The largest
202 number of DEGs was in this comparison. In the BA sample compared with the CA
203 sample, 281 genes were differentially expressed: 228 were upregulated and 53 were
204 downregulated.

205 ***Genes related to degradation of aromatic compounds***

206 The genes involved in the degradation of 3-CB and BA and the logFC differences in their
207 transcript levels between pairs of sample groups are shown in Table 1. The TPM values of
208 each gene are shown in Figure 2. *benABCD* genes (Fig. S2A) were highly expressed in
209 both the 3-CB and BA samples compared with the CA sample (logFC values 8.0 to 8.5).
210 This is reasonable because BenABCD enzymes presumably react with both 3-CB and BA
211 (Ogawa *et al*. 2003). The chlorocatechol-degradation genes *cbnABCD* (Fig. S2B) (Ogawa
212 and Miyashita 1999) were strongly induced in the 3-CB sample (logFC values 9.4 to 9.9)
213 but were not highly expressed in the BA sample (logFC values 1.3 to 1.5) as in the 3-CB
214 sample. The genes *catA* (Fig. S2A), *catB*, *catDC* (Fig. S2C), and *pcaIJF* (Fig. S2D)
215 encode products that participate in the degradation of catechol and 3-oxoadipate,
216 respectively, and were expressed at almost the same levels in the 3-CB and BA samples. A
217 Kyoto Encyclopedia of Genes and Genomes (KEGG) pathway analysis revealed that NH9
218 is able to decompose BA via another pathway, the epoxybenzoyl-CoA pathway (Ismail

219 and Gescher 2012), encoded by *bclA* and *boxABCD* genes (Fig. S2E and F). The
220 *boxABCD* genes were upregulated in the BA sample compared with the CA sample.
221 However, the transcript levels of *boxABCD* genes were lower than those of *ben* and *cat*.

222 In our previous study, analyses of the genome sequence of strain NH9 revealed
223 genes involved in pathways that completely degrade 2-hydroxybenzoate (2-HBA), 3-
224 hydroxybenzoate (3-HBA) (Fig. S2G), or 4-HBA (Fig. S2H) (Moriuchi *et al*. 2019). The
225 transcript levels of the genes that putatively degrade these aromatic compounds were
226 determined to ascertain whether 3-CB and BA affect their expression (Fig. S3 and Table
227 S2). The transcript levels of the genes involved in the degradation of 2-HBA or 4-HBA
228 were not very different between the CA sample and the 3-CB and BA samples (only *pobA*
229 in the BA sample was highly induced). Interestingly, the genes involved in the degradation
230 of 3-HBA in NH9 (renamed from *nag* to *mhb*) (Moriuchi *et al*. 2019) were significantly
231 induced only by 3-CB.

232 Strain NH9 has genes related to anthranilate degradation on chromosome 1
233 (designated as *and1* or *andAc1Ad1Ab1Aa1*) (Fig. S2I). The products of those genes
234 exhibit 43.9% to 73.3% amino acid sequence identities with the corresponding subunits of
235 AndAcAdAbAa from *Burkholderia cepacia* DBO1, which is regulated by an AraC/XylS-
236 type transcriptional regulator (Chang *et al*. 2003) (Fig. S4A). Like the *mhb* genes above,
237 *and1* was induced by 3-CB to a transcript level 8-fold that in the BA and CA samples
238 (Fig. S3 and Table S2). Chromosome 2 also harbors putative *and* genes (designated as
239 *and2* or *andAc2Ad2Ab2Aa2*) (Fig. S2J) and their transcript levels were significantly
240 higher in the 3-CB sample than in the BA sample (Table S3). However, their amino acid
241 sequence identities with the corresponding subunit of AndAcAdAbAa from *B. cepacia*
242 DBO1 were found to be lower than 45% (Fig. S4A). Also, the putative transcriptional

243 regulator located close to the degradation genes was a member of the MarR family, rather
244 than being an AraC/XylS-type regulator. Therefore, it is difficult to speculate whether
245 *and2* genes are involved in anthranilate degradation or not.

246 ***Transporters***

247 The KEGG BRITE functional classification of strain NH9 revealed that 348 genes encode
248 proteins with transporting functions ("Transporters," ko02000). Of these 348 genes, those
249 that were upregulated (logFC ≥ 2 and FDR < 0.05) by 3-CB and/or BA encoded eight
250 major facilitator superfamily (MFS) transporters and 12 sets of ATP-binding cassette
251 (ABC) transporters. This analysis identified the transporters induced by 3-CB and/or BA
252 (Table 2).

253 Of the eight MFS transporter genes mentioned above, BJN34_12320,
254 BJN34_18155, and BJN34_30890 had higher transcript levels in the 3-CB sample than in
255 the BA sample, and BJN34_32125 showed the opposite result. The logFC values of the
256 other four genes were not significantly different between 3-CB vs. CA and BA vs. CA. A
257 BLASTP analysis was performed to compare the amino acid sequences of the eight
258 transporters of NH9 with those that have been experimentally verified or functionally
259 analyzed (Table S4). The products of BJN34_18155 and BJN34_32125 exhibited more
260 than 70% amino acid sequence identities with BenP (a 3-CB transporter) (Ledger *et al*.
261 2009). The products of BJN34_30890 and BJN34_33870 showed moderate identities
262 (>50%) with MhbT (a 3-HBA transporter) (Xu *et al*. 2012) and PcaK (a 4-HBA
263 transporter) (Harwood *et al*. 1994; Nichols and Harwood 1997), respectively (Table 2).
264 Phylogenetic analysis of the eight MFS transporters of NH9 together with other known
265 MFS transporters confirmed the close relationships of the four transporters mentioned
266 above with their counterparts in other species, and grouped them in the aromatic acid:H^+

267 symporter (AAHS) family of MFS (Fig. 3). Three other transporters (products of
268 BJN34_11715, BJN34_12320, and BJN34_26825) belonged to the anion/cation symporter
269 (ACS) family and the product of BJN34_20520 belonged to the metabolite:H^+ symporter
270 (MHS) family. We then explored the genes surrounding the eight MFS transporter-
271 encoding genes in the NH9 genome, and found that BJN34_32125, BJN34_30890,
272 BJN34_33870, and BJN34_18155 were located next to clusters of genes related to the
273 degradation of BA, 3-HBA, 4-HBA, and anthranilate, respectively (Fig. S2F, G, H, and I).
274 No clusters of genes involved in degradation of aromatic compounds were located around
275 the genes encoding the other four MFS transporters.

276 Our results showed that 3-CB and BA induced many genes encoding ABC
277 transporters in NH9 (Table 2). The logFC values of most ABC transporter genes were
278 similar between 3-CB vs. CA and BA vs. CA. However, BJN34_29445 to BJN34_29465
279 were clearly overexpressed in the 3-CB sample, suggesting that these genes were induced
280 specifically by 3-CB. These gene products showed 27.7% to 40.3% amino acid sequence
281 identities with Pca proteins, which are involved in 3,4-dihydroxybenzoate transport
282 (MacLean *et al*. 2011). Transporters in other families were also identified in the BLASTP
283 analysis (Table S5). Although a few genes (e.g., BJN34_08680 and BJN34_26835) were
284 differentially expressed in response to both 3-CB and BA, most genes did not show
285 significant changes in their transcript levels, or were downregulated, in either the 3-CB or
286 BA samples compared with the CA sample.

287 ***Stress responses***

288 Stress response genes were upregulated when NH9 cells were cultured with 3-CB and BA
289 (Table S3). Four genes encoding molecular chaperones, *dnaK* (BJN34_09490), *groEL*
290 (BJN34_09495), *groES* (BJN34_09500), and *clpB* (BJN34_11475) were significantly

291 upregulated more than 2-fold by both 3-CB and BA compared with CA. *hslV*
292 (BJN34_00915), *hslU* (BJN34_00920), *grpE* (BJN34_06000), and *dnaK* (BJN34_16500)
293 were induced only by BA (FDR < 0.05). We also searched for the genes in strain NH9
294 corresponding to the aromatics stress response genes identified in the previous study
295 (Reva *et al*. 2006) in the KEGG database, and their expression patterns are summarized in
296 Table S3 (categorized as "Benzoate stress response genes"). Contrary to our expectation,
297 more than half of those genes were downregulated by 3-CB and BA compared with CA.
298 Only the genes encoding the phosphate transporter PstBACS (BJN34_13095 to
299 BJN34_13110) and superoxide oxidase (SOO) (BJN34_16665) were induced by 3-CB and
300 BA, respectively.

301 ***Functional changes***

302 To detect changes in biological function, we conducted GO enrichment analysis by the
303 PAGE method based on logFC values. The comparisons of 3-CB vs. CA, BA vs. CA, and
304 3-CB vs. BA detected enrichment of 22, 22, and 15 GO terms, respectively, with FDR <
305 0.05 (Fig. 4 and Table S6). The GO terms "ferric iron binding" (GO:0008199), "metal ion
306 binding" (GO:0046872), and "2 iron, 2 sulfur cluster binding" (GO:0051537) were
307 significantly upregulated only in the 3-CB sample. On the contrary, the GO terms
308 "nucleotide binding" (GO:0000166) and "peptidyl-prolyl cis-trans isomerase activity"
309 (GO:0003755) were significantly downregulated only in the 3-CB sample. In the BA
310 sample specifically, the GO terms "peptide transport" (GO:0015833) and "bacterial-type
311 flagellum-dependent cell motility" (GO:0071973) were significantly upregulated and
312 "GTPase activity" (GO:0003924), "porin activity" (GO:0015288), and "oxidoreductase
313 activity, acting on the CH-OH group of donors, NAD or NADP as acceptor"
314 (GO:0016616) were significantly downregulated. Interestingly, "chemotaxis"

315 (GO:0006935), “signal transduction” (GO:0007165), and “bacterial-type flagellum-
316 dependent cell motility” (GO:0071973) were downregulated in the 3-CB sample
317 compared with the BA sample, suggesting that the cell motility or chemotaxis of strain
318 NH9 was stronger towards BA than towards 3-CB. The trends in the variations of the
319 other GO terms listed in Fig. 4 and Table S6 were similar between 3-CB vs. CA and BA
320 vs. CA.

321 The induction or repression of genes in the “signal transduction,” “chemotaxis,” and
322 “bacterial-type flagellum-dependent cell motility” categories in response to 3-CB, BA,
323 and CA is summarized in Table S7. The 72 genes in the “signal transduction” category
324 mainly encoded proteins related to bacterial chemotaxis and a histidine kinase. Crucially,
325 this category included 12 genes encoding methyl-accepting chemotaxis proteins (MCPs),
326 which play key roles in sensing extracellular signals (Bi and Sourjik 2018; Parales *et al*.
327 2015). Eight of 12 MCP genes were DEGs in the 3-CB vs. BA comparison, and were
328 downregulated in the 3-CB sample. Because three of these eight genes (BJN34_09575,
329 BJN34_21800, and BJN34_32190) were upregulated more than 2-fold with FDR < 0.05
330 by BA compared with CA, it is likely that their products detect BA or related chemicals as
331 ligands. One MCP gene (BJN34_24350) was significantly upregulated more than 16-fold
332 by both 3-CB and BA compared with CA, indicating that it responded to 3-CB and BA or
333 their related chemicals. In the “chemotaxis” category, many genes were classified as
334 “signal transduction.” Seven of 16 genes were DEGs in the 3-CB vs. BA comparison, and
335 six of them were upregulated more than 2-fold (FDR < 0.05) by BA compared with CA.
336 These six genes encoded CheABDVW proteins and a MCP. Of the 14 genes in the
337 “bacterial-type flagellum-dependent cell motility” category, 11 were upregulated more
338 than 2-fold (FDR < 0.05) by BA compared with CA. These genes encoded proteins

339 comprising the flagellum: the hook, hook-filament junction, distal rod, proximal rod, L
340 ring, P ring, and a part of the C ring. Our data indicated that the genes encoding MCP,
341 Che, and components of the flagellum in NH9 were upregulated by BA and
342 downregulated or not affected by 3-CB. This was predicted to result in differences in cell
343 motility or chemotaxis functions of NH9 cells between 3-CB and BA.

344 ***Chemotactic response toward aromatic compounds***

345 To determine whether the transcriptional responses of chemotaxis genes corresponded to
346 actual differences in chemotaxis behavior towards 3-CB and BA, we performed semi-solid
347 agar plate assays (Fig. 5). The formation of a concentric ring was a positive response, as it
348 was indicative of the accumulation of bacterial cells encircling the attractant. NH9 cells
349 formed clear migrating rings around casamino acids (positive control) and BA within 3
350 and 6 h, respectively (Fig. 5A and B). In contrast, NH9 cells formed a migrating ring only
351 weakly around 3-CB after 14 h (Fig. 5C). There was no ring around BSM without any
352 carbon source (negative control) (Fig. 5D). These results confirmed that strain NH9 has a
353 strong chemotactic response towards BA but a weak response towards 3-CB.

354 **Discussion**

355 In this study, the results of transcriptome analysis of the cells of NH9 grown with 3-CB,
356 BA, and CA showed differential expression patterns depending on the substrate. While the
357 expression patterns of the genes involved in the degradation of 3-CB and BA were highly
358 upregulated in agreement with our expectation, some of the genes involved in transport
359 and chemotaxis were differentially regulated between 3-CB and BA, which suggested
360 different level of adaptation of NH9 to the two compounds (see below).

361 The RNA-seq analyses confirmed that genes related to 3-CB and BA metabolism
362 are expressed in NH9, as predicted in a previous study (Moriuchi *et al*. 2019). The
363 *cbnABCD* genes encoding enzymes involved in 3-chlorocatechol degradation were
364 upregulated in NH9 cells grown with 3-CB and BA, especially 3-CB (Table 1 and Fig. 2).
365 In NH9 cells grown with 3-CB and BA, *benABCD* and *catA* were upregulated, presumably
366 as a result of the action of the LysR-type transcriptional regulator (BJN34_08550) (Fig.
367 S2A). These results are consistent with the degradation pathways of the two compounds.
368 *catB* and *catDC* were upregulated in NH9 cells in the presence of either 3-CB or BA and
369 are located on a different chromosome from *benABCD* and *catA.* While the expression of
370 the *catB* gene could be regulated by the product of BJN34_24335 encoding a LysR-type
371 transcriptional regulator, a transcriptional regulator of *catDC* genes could not be estimated
372 (Fig. S2C). The *boxABCD* genes encoding enzymes involved in BA degradation were
373 upregulated in BA compared with CA, but the transcript levels of them were lower than
374 those of *ben* and *cat* genes (Table 1 and Fig. 2). These results suggested that, in these
375 experimental conditions, NH9 may primarily degrade BA via the route involving *ben* and
376 *cat* genes, rather than the route involving *bclA* and *boxABCD* genes. In other conditions,
377 such as lower oxygen levels or growth on other carbon sources, expression of *bclA* and
378 *boxABCD* genes may be higher than that of *ben* and *cat* genes as reported in *P.*
379 *xenovorans* LB400 (Denef *et al*. 2004, 2006).

380 *C. necator* NH9 consumed both 3-CB and BA within 18 h, when growth
381 apparently reached the stationary phase (Fig. 1). However, even after aromatic compounds
382 were completely degraded, the OD_{600} of the culture did not decrease during a further 30 h.
383 When strain NH9 was cultured with CA, the curve showed a similar trend. This is
384 probably due to the accumulation and consumption of the biodegradable polyester,

385 polyhydroxybutyrate (PHB). PHB is naturally synthesized as a carbon reserve storage
386 material from acetyl-CoA, which is metabolite of both 3-CB and BA, under nutrient
387 limitation and stress conditions (Chen 2009). *Cupriavidus necator* strain H16 has been
388 studied intensively as a PHB producer. The genome of H16 contains classic PHB
389 synthesis genes ($phaC_1AB_1$ operon) that are distributed and conserved among members of
390 the genus *Cupriavidus* (Kutralam-Muniasamy and Peréz-Guevara 2018; Peoples and
391 Sinskey 1989). The genome of strain NH9 also contains *pha* genes (Table S3). The
392 proteins encoded by these genes showed more than 93% amino acid identities with those
393 of H16. In the present study, these *pha* genes were expressed at higher levels than the
394 median TPM values of all genes (3-CB_1: 31.3, 3-CB_2: 30.3, 3-CB_3: 26.0, BA_1: 29.5,
395 BA_2: 26.1, BA_3: 29.9, CA_1: 15.4, CA_2: 20.5, and CA_3: 20.1), regardless of the
396 substrate, suggesting that PHB synthesis occurred under these conditions.

397 The products of *mhbDHIMT* genes in strain NH9 showed high identities (52.1%
398 to 71.9% identity at the amino acid level) with those involved in the degradation of 3-
399 HBA in *Klebsiella pneumoniae* M5a1 (Fig. S4B). A previous study on strain M5a1
400 reported that the expression of *mhb* degradation genes is regulated by *mhbR* (located
401 upstream), which is induced by 3-HBA (Lin *et al*. 2010). We conducted growth
402 experiments and qRT-PCR analyses of NH9 cells grown with 3-HBA as the substrate and
403 obtained the following results: (i) NH9 cells were able to use 3-HBA as the sole source of
404 carbon and energy; and (ii) the *mhbDHIMT* genes in NH9 were highly induced by 3-HBA
405 (data not shown). These results strongly suggest that *mhbDHIMT* genes in strain NH9 are
406 involved in the degradation of 3-HBA and are induced by 3-HBA, consistent with the *mhb*
407 genes in *K. pneumoniae* M5a1. In this study, 3-CB was found to upregulate the expression
408 of *mhbDHIMT* genes in strain NH9 (Fig. S3 and Table S2). Thus our results imply that

409 MhbR in NH9 recognized not only 3-HBA but also 3-CB (or its intermediate metabolite)
410 as an inducer to activate the transcription of *mhbDHIMT* genes. Strain NH9 harbors
411 putative anthranilate decomposition genes on chromosome 1 (*and1*) and chromosome 2
412 (*and2*), and these genes were also upregulated by 3-CB but not by BA (Fig. S3, Tables S2,
413 and S3). The presence of the complete set of genes for the initial degradation of
414 anthranilate, together with *andR* encoding an AraC/XylS-type transcriptional regulator
415 located upstream of the *and1* genes, suggests that *and1* gene cluster is functional.
416 Although anthranilate is structurally more different from 3-CB than 3-HBA is, the
417 transcriptional regulator of anthranilate degradation genes in NH9 may recognize 3-CB (or
418 its intermediate metabolite) as an inducer.

419 Many candidate genes involved in the transport of 3-CB and/or BA were
420 identified via the KEGG BRITE functional classification and BLASTP analyses (Tables 2
421 and S5). Because BJN34_18155 and BJN34_32125 are evolutionarily close to BenP, a
422 MFS transporter involved in 3-CB uptake in *C. pinatubonensis* JMP134 (Ledger *et al.*
423 2009) (Fig. 3), their products may be involved in 3-CB import in NH9. BJN34_18155,
424 BJN34_30890, BJN34_32125, and BJN34_33870, which encode MFS transporters, may
425 be involved in the transport of anthranilate, 3-HBA, BA, and 4-HBA, respectively,
426 because each of these genes is located in a cluster of genes related to degradation of each
427 respective compound (Fig. S2F, G, H, and I). Genes encoding components of the ABC
428 transport system (BJN34_29445 to BJN34_29465) were more strongly expressed in NH9
429 cells grown with 3-CB than in NH9 cells grown with BA or CA. As far as we know, the
430 ABC transporter that imports 3-CB into cytoplasm has not been reported yet. The products
431 of BJN34_29445 to BJN34_29465 may be components of a novel 3-CB transporter.
432 Intriguingly, a gene related to anthranilate degradation (*and2*) was located next to

433 BJN34_29445 to BJN34_29465, and was significantly induced by 3-CB (Fig. S2J and
434 Table S3). Thus, this ABC transporter system may be originally involved in importing
435 anthranilate. Aromatic compounds are taken up by members of the MFS and ABC
436 families, but also by members of other transporter families (Chae and Zylstra 2006;
437 Hosaka *et al*. 2013; Olivera *et al*. 1998; Reverón *et al*. 2017). However, our results
438 indicate that the MFS and ABC family transporters listed in Table 2 could play key roles
439 in importing 3-CB and BA into NH9 cells.

440 The stress response genes with altered expression included those encoding
441 molecular chaperones (DnaK, GrpE, GroESL, and ClpB) and proteases (HslVU) (Table
442 S3). Previous studies have shown that these proteins are rapidly induced under various
443 stress conditions such as salt, acid, heat, cold and oxidative stress (Gaucher *et al*. 2019). In
444 NH9, genes encoding either chaperones or proteases might be upregulated to refold
445 misfolded proteins and to decrease the harmful impact of protein aggregation in the
446 presence of aromatic compounds (Table S3). In another study, the stress responses of *P*.
447 *putida* KT2440 to 45 mM BA were analyzed by global mRNA expression profiling and
448 several genes were identified as stress response genes (Reva *et al*. 2006). We expected that
449 the genes induced by BA in strain KT2440 are also upregulated by 3-CB and/or BA in
450 strain NH9, however expression of more than half of investigated genes (BJN34_02220,
451 BJN34_03315, BJN34_03320, BJN34_15890, BJN34_16755, BJN34_23155, and
452 BJN34_25760) appeared to be relatively low in 3-CB and BA compared with CA (Table
453 S3). Although the TPM values of five of the seven genes (BJN34_02220 encoding
454 protoheme IX farnesyltransferase, BJN34_03315 and BJN34_03320 encoding succinyl-
455 CoA synthetase, BJN34_15890 encoding TonB-dependent receptor, and BJN34_16755
456 encoding outer membrane protein assembly factor) were highest in CA (data not shown),

457 the TPM values of the five genes in both 3-CB and BA were higher than the median TPM
458 values of all genes. This suggested that, while the five genes were expressed in 3-CB and
459 BA, NH9 cells suffered most severe stress in CA in which the cells of NH9 exhibited the
460 fastest growth rate among the three conditions. The nature of the stress caused by growth
461 in CA remains to be solved. Genes encoding the phosphate transporter PstBACS and
462 superoxide scavenger SOO (Lundgren *et al*. 2018) were also induced by 3-CB and BA,
463 respectively in NH9. The previous study estimated that intracellular phosphate is a buffer
464 for neutralizing the BA and is used in the synthesis of membrane constituents and energy-
465 rich intermediates (Reva *et al*. 2006). Presumably, PstBACS coding genes might be
466 upregulated to maintain the intracellular pH disturbed by 3-CB. The degradation of
467 aromatic compounds by oxygenases can generate reactive oxygen species (ROS) which
468 damage various cellular components such as DNA, proteins, and lipid in aerobic
469 organisms (Flood and Copley 2018; Tamburro *et al*. 2004) and upregulate various stress
470 response genes (Chávez *et al*. 2004; Denef *et al*. 2006; Puglisi *et al*. 2010; Wang *et al*.
471 2011). This study suggested that SOO coding genes were also induced to solve ROS
472 accumulation. The incorporation and aerobic degradation of 3-CB and BA could cause
473 stress conditions including changes in intracellular pH and ROS accumulation. In the
474 previous transcriptomic studies of *P*. *putida* KT2440 and *P*. *xenovorans* LB400, a variety
475 of stress response genes were found to be upregulated by 3-CB and BA, and by BA,
476 biphenyl, and PCBs, respectively (Denef *et al*. 2006; Parnell *et al*. 2006; Reva *et al*. 2006;
477 Wang *et al*. 2011). The results obtained in this study were consistent with those of the
478 previous studies above in that chlorinated aromatic compounds or analogous aromatic
479 compounds induced the expression of genes involved in pH and oxidative stresses.

480 The four GO terms, “cellular aromatic compound metabolic process,” “iron ion
481 binding,” “2 iron, 2 sulfur cluster binding,” and “ferric ion binding” were upregulated by
482 3-CB and BA compared with CA. In particular, 3-CB induced the expression of many
483 genes encoding dioxygenases (Fig. 4 and Table S6). Dioxygenases contain two conserved
484 regions: the Rieske [2Fe-2S] cluster and the mononuclear iron-containing catalytic
485 domain. These enzymes play a critical role in initiating the biodegradation of a variety of
486 aromatic compounds under aerobic conditions (Mason and Cammack 1992). Upregulation
487 of these functions, including dioxygenase activity, would be conducive to the degradation
488 of aromatic pollutants.

489 Notably, NH9 cells showed stronger chemotaxis towards BA than towards 3-CB,
490 as demonstrated in the semi-solid agar plate assays (Fig. 5). This was consistent with the
491 upregulation of chemotaxis genes by BA compared with 3-CB. The predicted chemotaxis
492 pathway of strain NH9 towards BA is described below and depicted in Fig. 6. To initiate
493 the typical chemotactic response, MCPs first detect their ligands (Parales *et al*. 2015). In
494 strain NH9, among 12 genes encoding MCPs, at least four, BJN34_09575 (K05874),
495 BJN34_21800 (K05874), BJN34_24350 (K05874), and BJN34_32190 (K03406), encode
496 products that could function as receptors for BA or related chemicals. Binding of an
497 attractant induces a conformational change in MCPs such that they transfer a phosphate
498 group from the histidine kinase CheA (BJN34_21875) to the response regulator CheY (Bi
499 and Sourjik 2018). The NH9 genome contains two *cheY* genes (BJN34_21830 and
500 BJN34_21900) that were significantly upregulated by BA and downregulated by 3-CB
501 (data not shown). The phosphorylated CheY interacts with switch proteins in the flagellar
502 motor such as FliM (BJN34_24450) (Welch *et al*. 1993), FliN (BJN34_24445) (Sarkar *et*
503 *al*. 2010) and FliG (BJN34_34155) (Nishikino *et al*. 2018). As a result, the swimming

504 behavior of bacterial cells migrates towards BA. The upregulation of the complete set of
505 genes required for chemotaxis strongly suggests that their products are involved in
506 chemotaxis to BA.

507 Among the few transporters reported to transport of chlorinated aromatic
508 compounds, TfdK of *C. pinatubonensis* JMP134 is encoded by a gene located at the
509 downstream end of a gene cluster involved in 2,4-D degradation. This protein is reported
510 to be involved in both the uptake of, and chemotaxis to, 2,4-D (Hawkins and Harwood
511 2002; Leveau *et al*. 1998). This tendency for genes with related functions to cluster
512 together is considered to be the result of evolution (Reams and Neidle 2004). It has been
513 observed for many genes encoding MFS transporters of aromatic compounds commonly
514 found in nature, for example, *pcaK,* which is involved in the uptake of, and chemotaxis to,
515 4-HBA in *P. putida* (Luu *et al*. 2015), and *benK,* which is involved in the uptake of BA in
516 *Acinetobacter baylyi* ADP1 (Collier *et al*. 1997). In contrast, the genes involved in uptake
517 of/chemotaxis to 3-CB in bacteria have remained elusive. That is, the genes that are
518 presumed to be responsible for these functions are not located adjacent to genes involved
519 in 3-CB degradation (encoding front-end enzymes, benzoate 1,2-dioxygenase and *cis*-diol
520 dehydrogenase, and enzymes involved in chlorocatechol *ortho*-cleavage pathway). *C.*
521 *pinatubonensis* strain JMP134 utilizes 3-CB as well as 2,4-D. However, in strain JMP134,
522 *benP* (encoding a protein involved in 3-CB uptake) is not located on the plasmid pJP4 that
523 contains genes related to the degradation of 2,4-D and chlorocatechols converted from 3-
524 CB, but is located on the chromosome (Ledger *et al*. 2009). With regard to chemotaxis to
525 3-CB, the presence of ICE*clc* in strain B13 was found to be related to the upregulation of
526 genes involved in flagellar assembly and increased swimming motility (Miyazaki *et al*.
527 2018). A B13 strain that did not contain ICE*clc*, but only the chlorocatechol degradation

528 genes, did not show upregulation of swimming motility. The upregulation in the ICE*clc*-
529 containing strain was suggested to be mediated by a gene located in ICE*clc*, *orf2848*,
530 which is homologous to *pcaK* (Miyazaki *et al*. 2018). In the present study, the genes
531 encoding transporters that were upregulated by 3-CB were located on chromosomes either
532 discretely or together with genes related to the degradation of aromatic compounds such as
533 3-HBA and anthranilate (Fig. S2G, I, and J), but were not closely located to genes
534 involved in 3-CB degradation (encoding the front-end enzymes and the enzymes for
535 chlorocatechol degradation). This raises several possibilities: 1. Utilization of 3-CB does
536 not require increased expression of specific transporter (s), and the transporter genes that
537 were upregulated in NH9 cells grown with 3-CB were fortuitously upregulated. 2. While
538 3-CB strongly induces genes encoding front-end enzymes including benzoate 1,2-
539 dioxygenase, the gene (s) related to BA uptake are insufficient for 3-CB uptake.
540 Therefore, other transporter genes, such as those upregulated in our study, are induced to
541 complement this function. Because the substrate specificity of aromatic compound
542 transporters is not known, either of these possibilities may explain the uptake of 3-CB.
543 However, if we include chemotaxis (which may be linked to uptake) when considering the
544 behavior of NH9 towards 3-CB (Fig. 5), our results show that NH9 has weaker
545 chemotaxis towards 3-CB than towards BA. This fact, combined with the absence of
546 closely located genes related to uptake/chemotaxis, strongly suggests that strain NH9 does
547 not utilize 3-CB as efficiently as it utilizes BA in the environment. In our experiments,
548 NH9 also showed strong chemotaxis towards 3-HBA (data not shown), providing further
549 evidence that this strain is adapted for utilization of aromatic compounds commonly found
550 in nature.

551 **Conclusion**

552 We examined transcriptome differences in *C. necator* strain NH9 between cells cultured
553 with 3-CB and those cultured with BA. The RNA-seq analyses revealed more changes in
554 gene expression in response to 3-CB than to BA. The trends in differential gene
555 expression were similar, but genes related to the degradation of particular aromatic
556 compounds (3-chlorocatechol, BA, 3-HBA, and anthranilate) showed differences in
557 transcript levels among the various treatments. The genes encoding transporters (MFS and
558 ABC type), components of the stress response, flagellar proteins, and chemotaxis proteins
559 also showed differences between 3-CB and BA. The chemotaxis response of NH9 cells
560 showed the biggest difference between 3-CB and BA. The substrate BA markedly
561 upregulated certain genes related to the chemotaxis response, but 3-CB did not, consistent
562 with the chemotaxis behavior observed in semi-solid agar assays. Together, our findings
563 suggest that NH9 has not fully adapted to utilization of chlorinated benzoate, unlike its
564 analogous aromatic compounds such as BA.

565 **Abbreviations**

566 2,4-D, 2,4-dichlorophenoxyacetic acid; 3-CB, 3-chlorobenzoate; AAHS, aromatic acid:H^+
567 symporter; ABC, ATP-binding cassette; ACS, anion/cation symporter; BA, benzoate;
568 BSM, basal salts medium; CA, citric acid; DEGs, differentially expressed genes; FDR,
569 false discovery rate; GO, gene ontology; HBA, hydroxybenzoate; HPLC, high
570 performance liquid chromatography; KEGG, Kyoto Encyclopedia of Genes and Genomes;
571 LogFC, log fold-change; MCP, methyl-accepting chemotaxis protein; MDS, multi-
572 dimensional scaling; MFS, major facilitator superfamily; MHS, metabolite:H^+ symporter;
573 OD_{600}, optical density at 600 nm; PAGE, parametric analysis of gene set enrichment;
574 PCBs, polychlorinated biphenyls; PHB, polyhydroxybutyrate; ROS, reactive oxygen
575 species; SOO, superoxide oxidase; TPM, transcripts per million.

576 **Acknowledgements**

577 The authors thank Mr. Ayumu Wada (Nippon Paper Industries Co., Ltd.) for his valuable
578 comments. We also thank Dr. Kimiko Yamamoto-Tamura (Institute for Agro-
579 Environmental Sciences, NARO) for her helpful advice for the semi-solid agar plate
580 assay.

581 **Author contributions**

582 RM and NO conceived and designed the experiments. RM performed the experiments,
583 analyzed and interpreted the data, and wrote the manuscript. HD and YK provided
584 assistance with analytical tools. HD, YK, and NO critically reviewed the manuscript. NO
585 is responsible for the project.

586 **Disclosure statement**

587 No potential conflict of interest was reported by the authors.

588 **Data availability**

589 Raw data sequences generated in the current study have been submitted to the DDBJ
590 Sequence Read Archive (DRA) under the accession no. DRR232374 to DRR232382.

591 **Funding**

592 This work was partially supported by JSPS KAKENHI (Grant-in-Aid for Scientific
593 Research (C)), grant number 26450087.

594 **Statement of ethics**

595 This research did not require ethical approval.

596 **References**

597 Alexander M. Biodegradation of chemicals of environmental concern. *Science* 1981;211(4478):132-8.

598 Ashburner M, Ball CA, Blake JA *et al*. Gene ontology: tool for the unification of biology. *Nat Genet*
599 2000;25(1):25-9.

600 Bi S, Sourjik V. Stimulus sensing and signal processing in bacterial chemotaxis. *Curr Opin Microbiol*
601 2018;45:22-9.

602 Bolger AM, Lohse M, Usadel B. Trimmomatic: a flexible trimmer for Illumina sequence data.
603 *Bioinformatics* 2014;30(15):2114-20.

604 Bott TL, Kaplan LA. Autecological properties of 3-chlorobenzoate-degrading bacteria and their
605 population dynamics when introduced into sediments. *Microb Ecol* 2002;43(2):199-216.

606 Chae JC, Zylstra GJ. 4-chlorobenzoate uptake in *Comamonas* sp. strain DJ-12 is mediated by a
607 tripartite ATP-independent periplasmic transporter. *J Bacteriol* 2006;188(24):8407-12.

608 Chang HK, Mohseni P, Zylstra GJ. Characterization and regulation of the genes for a novel anthranilate
609 1,2-dioxygenase from *Burkholderia cepacia* DBO1. *J Bacteriol* 2003;185(19):5871-81.

610 Chávez FP, Lünsdorf H, Jerez CA. Growth of polychlorinated-biphenyl-degrading bacteria in the
611 presence of biphenyl and chlorobiphenyls generates oxidative stress and massive accumulation of
612 inorganic polyphosphate. *Appl Environ Microbiol* 2004;70(5):3064-72.

613 Chen GQ. A microbial polyhydroxyalkanoates (PHA) based bio- and materials industry. *Chem Soc Rev*
614 2009;38(8):2434-46.

615 Collier LS, Nichols NN, Neidle EL. *benK* encodes a hydrophobic permease-like protein involved in
616 benzoate degradation by *Acinetobacter* sp. strain ADP1. *J Bacteriol* 1997;179(18):5943-6.

617 Denef VJ, Klappenbach JA, Patrauchan MA *et al*. Genetic and genomic insights into the role of
618 benzoate-catabolic pathway redundancy in *Burkholderia xenovorans* LB400. *Appl Environ*
619 *Microbiol* 2006;72(1):585-95.

620 Denef VJ, Park J, Tsoi TV *et al*. Biphenyl and benzoate metabolism in a genomic context: outlining
621 genome-wide metabolic networks in *Burkholderia xenovorans* LB400. *Appl Environ Microbiol*
622 2004;70(8):4961-70.

623 Dennis P, Edwards EA, Liss SN *et al*. Monitoring gene expression in mixed microbial communities by
624 using DNA microarrays. *Appl Environ Microbiol* 2003;69(2):769-78.

625 Fang L, Shi T, Chen Y *et al*. Kinetics and catabolic pathways of the insecticide chlorpyrifos, annotation
626 of the degradation genes, and characterization of enzymes TcpA and Fre in *Cupriavidus*
627 *nantongensis* X1^{T}. *J Agric Food Chem* 2019;67(8):2245-54.

628 Fida TT, Moreno-Forero SK, Breugelmans P *et al*. Physiological and transcriptome response of the
629 polycyclic aromatic hydrocarbon degrading *Novosphingobium* sp. LH128 after inoculation in soil.
630 *Environ Sci Technol* 2017;51(3):1570-9.

631 Flood JJ, Copley SD. Genome-wide analysis of transcriptional changes and genes that contribute to
632 fitness during degradation of the anthropogenic pollutant pentachlorophenol by *Sphingobium*
633 *chlorophenolicum*. *mSystems* 2018;3(6).

634 Gaucher F, Bonnassie S, Rabah H *et al*. Review: Adaptation of beneficial propionibacteria, lactobacilli,
635 and bifidobacteria improves tolerance toward technological and digestive stresses. *Front Microbiol*
636 2019;10:841.

637 Gibson J, Harwood CS. Metabolic diversity in aromatic compound utilization by anaerobic microbes.
638 *Annu Rev Microbiol* 2002;56:345-69.

639 Gonçalves ER, Hara H, Miyazawa D *et al*. Transcriptomic assessment of isozymes in the biphenyl
640 pathway of *Rhodococcus* sp. strain RHA1. *Appl Environ Microbiol* 2006;72(9):6183-93.

641 Hara H, Eltis LD, Davies JE *et al*. Transcriptomic analysis reveals a bifurcated terephthalate
642 degradation pathway in *Rhodococcus* sp. strain RHA1. *J Bacteriol* 2007;189(5):1641-7.

643 Harwood CS, Nichols NN, Kim MK *et al*. Identification of the *pcaRKF* gene cluster from
644 *Pseudomonas putida*: involvement in chemotaxis, biodegradation, and transport of 4-
645 hydroxybenzoate. *J Bacteriol* 1994;176(21):6479-88.

646 Hawkins AC, Harwood CS. Chemotaxis of *Ralstonia eutropha* JMP134(pJP4) to the herbicide 2,4-
647 dichlorophenoxyacetate. *Appl Environ Microbiol* 2002;68(2):968-72.

648 Hosaka M, Kamimura N, Toribami S *et al*. Novel tripartite aromatic acid transporter essential for
649 terephthalate uptake in *Comamonas* sp. strain E6. *Appl Environ Microbiol* 2013;79(19):6148-55.

650 Iino T, Wang Y, Miyauchi K *et al*. Specific gene responses of *Rhodococcus jostii* RHA1 during growth
651 in soil. *Appl Environ Microbiol* 2012;78(19):6954-62.

652 Imperlini E, Bianco C, Lonardo E *et al*. Effects of indole-3-acetic acid on *Sinorhizobium meliloti*
653 survival and on symbiotic nitrogen fixation and stem dry weight production. *Appl Microbiol*
654 *Biotechnol* 2009;83(4):727-38.

655 Ismail W, Gescher J. Epoxy coenzyme A thioester pathways for degradation of aromatic compounds.
656 *Appl Environ Microbiol* 2012;78(15):5043-51.

657 Ito N, Itakura M, Eda S *et al*. Global gene expression in *Bradyrhizobium japonicum* cultured with
658 vanillin, vanillate, 4-hydroxybenzoate and protocatechuate. *Microbes Environ* 2006;21(4):240-50.

659 Kim D, Langmead B, Salzberg SL. HISAT: a fast spliced aligner with low memory requirements. *Nat*
660 *Methods* 2015;12(4):357-60.

661 Kim SY, Volsky DJ. PAGE: parametric analysis of gene set enrichment. *BMC Bioinformatics*
662 2005;6:144.

663 Kumar S, Stecher G, Tamura K. MEGA7: Molecular Evolutionary Genetics Analysis Version 7.0 for
664 Bigger Datasets. *Mol Biol Evol* 2016;33(7):1870-4.

665 Kutralam-Muniasamy G, Peréz-Guevara F. Genome characteristics dictate poly-R-(3)-
666 hydroxyalkanoate production in *Cupriavidus necator* H16. *World J Microbiol Biotechnol*
667 2018;34(6):79.

668 Ledger T, Aceituno F, Gonzalez B. 3-chlorobenzoate is taken up by a chromosomally encoded
669 transport system in *Cupriavidus necator* JMP134. *Microbiology* 2009;155(Pt 8):2757-65.

670 Leveau JH, Zehnder AJ, van der Meer JR. The *tfdK* gene product facilitates uptake of 2,4-
671 dichlorophenoxyacetate by *Ralstonia eutropha* JMP134(pJP4). *J Bacteriol* 1998;180(8):2237-43.

672 Lin LX, Liu H, Zhou NY. MhbR, a LysR-type regulator involved in 3-hydroxybenzoate catabolism via
673 gentisate in *Klebsiella pneumoniae* M5a1. *Microbiol Res* 2010;165(1):66-74.

674 Lundgren CAK, Sjöstrand D, Biner O *et al*. Scavenging of superoxide by a membrane-bound
675 superoxide oxidase. *Nat Chem Biol* 2018;14(8):788-93.

676 Luu RA, Kootstra JD, Nesteryuk V *et al*. Integration of chemotaxis, transport and catabolism in
677 *Pseudomonas putida* and identification of the aromatic acid chemoreceptor PcaY. *Mol Microbiol*
678 2015;96(1):134-47.

679 MacLean AM, Haerty W, Golding GB *et al*. The LysR-type PcaQ protein regulates expression of a
680 protocatechuate-inducible ABC-type transport system in *Sinorhizobium meliloti*. *Microbiology*
681 2011;157(Pt 9):2522-33.

682 Mason JR, Cammack R. The electron-transport proteins of hydroxylating bacterial dioxygenases. *Annu*
683 *Rev Microbiol* 1992;46:277-305.

684 Mitchell A, Chang HY, Daugherty L *et al*. The InterPro protein families database: the classification
685 resource after 15 years. *Nucleic Acids Res* 2015;43:D213-21.

686 Miyakoshi M, Shintani M, Terabayashi T *et al*. Transcriptome analysis of *Pseudomonas putida*
687 KT2440 harboring the completely sequenced IncP-7 plasmid pCAR1. *J Bacteriol*
688 2007;189(19):6849-60.

689 Miyazaki R, Yano H, Sentchilo V *et al*. Physiological and transcriptome changes induced by
690 *Pseudomonas putida* acquisition of an integrative and conjugative element. *Sci Rep* 2018;8(1):5550.

691 Moriuchi R, Dohra H, Kanesaki Y *et al*. Complete genome sequence of 3-chlorobenzoate-degrading
692 bacterium *Cupriavidus necator* NH9 and reclassification of the strains of the genera *Cupriavidus*
693 and *Ralstonia* based on phylogenetic and whole-genome sequence analyses. *Front Microbiol*
694 2019;10:133.

695 Nichols NN, Harwood CS. PcaK, a high-affinity permease for the aromatic compounds 4-
696 hydroxybenzoate and protocatechuate from *Pseudomonas putida*. *J Bacteriol* 1997;179(16):5056-
697 61.

698 Nishikino T, Hijikata A, Miyanoiri Y *et al*. Rotational direction of flagellar motor from the
699 conformation of FliG middle domain in marine *Vibrio*. *Sci Rep* 2018;8(1):17793.

700 Ogawa N, McFall SM, Klem TJ *et al*. Transcriptional activation of the chlorocatechol degradative
701 genes of *Ralstonia eutropha* NH9. *J Bacteriol* 1999;181(21):6697-705.

702 Ogawa N, Miyashita K. Recombination of a 3-chlorobenzoate catabolic plasmid from *Alcaligenes*
703 *eutrophus* NH9 mediated by direct repeat elements. *Appl Environ Microbiol* 1995;61(11):3788-95.

704 Ogawa N, Miyashita K. The chlorocatechol-catabolic transposon Tn*5707* of *Alcaligenes eutrophus*
705 NH9, carrying a gene cluster highly homologous to that in the 1,2,4-trichlorobenzene-degrading
706 bacterium *Pseudomonas* sp. strain P51, confers the ability to grow on 3-chlorobenzoate. *Appl*
707 *Environ Microbiol* 1999;65(2):724-31.

708 Ogawa N, Miyashita K, Chakrabarty AM. Microbial genes and enzymes in the degradation of
709 chlorinated compounds. *Chem Rec* 2003;3(3):158-71.

710 Olivera ER, Miñambres B, García B *et al*. Molecular characterization of the phenylacetic acid catabolic
711 pathway in *Pseudomonas putida* U: the phenylacetyl-CoA catabolon. *Proc Natl Acad Sci USA*
712 1998;95(11):6419-24.

713 Parales RE, Luu RA, Hughes JG *et al*. Bacterial chemotaxis to xenobiotic chemicals and naturally-
714 occurring analogs. *Curr Opin Biotechnol* 2015;33:318-26.

715 Parnell JJ, Park J, Denef V *et al*. Coping with polychlorinated biphenyl (PCB) toxicity: Physiological
716 and genome-wide responses of *Burkholderia xenovorans* LB400 to PCB-mediated stress. *Appl*
717 *Environ Microbiol* 2006;72(10):6607-14.

718 Patrauchan MA, Parnell JJ, McLeod MP *et al*. Genomic analysis of the phenylacetyl-CoA pathway in
719 *Burkholderia xenovorans* LB400. *Arch Microbiol* 2011;193(9):641-50.

720 Peoples OP, Sinskey AJ. Poly-beta-hydroxybutyrate biosynthesis in *Alcaligenes eutrophus* H16.
721 Characterization of the genes encoding beta-ketothiolase and acetoacetyl-CoA reductase. *J Biol*
722 *Chem* 1989;264(26):15293-7.

723 Pérez-Pantoja D, Leiva-Novoa P, Donoso RA *et al*. Hierarchy of carbon source utilization in soil
724 bacteria: Hegemonic preference for benzoate in complex aromatic compound mixtures degraded by
725 *Cupriavidus pinatubonensis* strain JMP134. *Appl Environ Microbiol* 2015;81(12):3914-24.

726 Pertea M, Pertea GM, Antonescu CM *et al*. StringTie enables improved reconstruction of a
727 transcriptome from RNA-seq reads. *Nat Biotechnol* 2015;33(3):290-5.

728 Puglisi E, Cahill MJ, Lessard PA *et al*. Transcriptional response of *Rhodococcus aetherivorans* I24 to
729 polychlorinated biphenyl-contaminated sediments. *Microb Ecol* 2010;60(3):505-15.

730 Reams AB, Neidle EL. Selection for gene clustering by tandem duplication. *Annu Rev Microbiol*
731 2004;58:119-42.

732 Reineke, W. Development of hybrid strains for the mineralization of chloroaromatics by patchwork
733 assembly. *Annu Rev Microbiol* 1998;52:287-331.

734 Reva ON, Weinel C, Weinel M *et al*. Functional genomics of stress response in *Pseudomonas putida*
735 KT2440. *J Bacteriol* 2006;188(11):4079-92.

736 Reverón I, Jiménez N, Curiel JA *et al*. Differential gene expression by *Lactobacillus plantarum*
737 WCFS1 in response to phenolic compounds reveals new genes involved in tannin degradation. *Appl*
738 *Environ Microbiol* 2017;83(7).

739 Robinson MD, McCarthy DJ, Smyth GK. edgeR: a Bioconductor package for differential expression
740 analysis of digital gene expression data. *Bioinformatics* 2010;26(1):139-40.

741 Saitou N, Nei M. The neighbor-joining method: a new method for reconstructing phylogenetic trees.
742 *Mol Biol Evol* 1987;4(4):406-25.

743 Sarkar MK, Paul K, Blair D. Chemotaxis signaling protein CheY binds to the rotor protein FliN to
744 control the direction of flagellar rotation in *Escherichia coli*. *Proc Natl Acad Sci USA*
745 2010;107(20):9370-5.

746 Sun J, Pan L, Zhu L. Formation of hydroxylated and methoxylated polychlorinated biphenyls by
747 *Bacillus subtilis*: New insights into microbial metabolism. *Sci Total Environ* 2018;613-614:54-61.

748 Tamburro A, Robuffo I, Heipieper HJ *et al*. Expression of glutathione S-transferase and peptide
749 methionine sulphoxide reductase in *Ochrobactrum anthropi* is correlated to the production of
750 reactive oxygen species caused by aromatic substrates. *FEMS Microbiol Lett* 2004;241(2):151-6.

751 van der Meer JR, de Vos WM, Harayama S *et al*. Molecular mechanisms of genetic adaptation to
752 xenobiotic compounds. *Microbiol Rev* 1992;56(4):677-94.

753 Wang Y, Morimoto S, Ogawa N *et al*. A survey of the cellular responses in *Pseudomonas putida*
754 KT2440 growing in sterilized soil by microarray analysis. *FEMS Microbiol Ecol* 2011;78(2):220-32.

755 Welch M, Oosawa K, Aizawa S *et al*. Phosphorylation-dependent binding of a signal molecule to the
756 flagellar switch of bacteria. *Proc Natl Acad Sci USA* 1993;90(19):8787-91.

757 Wu Y, Mohanty A, Chia WS *et al*. Influence of 3-chloroaniline on the biofilm lifestyle of *Comamonas*
758 *testosteroni* and its implications on bioaugmentation. *Appl Environ Microbiol* 2016;82(14):4401-9.

759 Xiang S, Lin R, Shang H *et al*. Efficient degradation of phenoxyalkanoic acid herbicides by the alkali-
760 tolerant *Cupriavidus oxalaticus* strain X32. *J Agric Food Chem* 2020;68(12):3786-95.

761 Xu Y, Gao X, Wang SH *et al*. MhbT is a specific transporter for 3-hydroxybenzoate uptake by Gram-
762 negative bacteria. *Appl Environ Microbiol* 2012;78(17):6113-20.

763 Yamamoto-Tamura K, Kawagishi I, Ogawa N *et al*. A putative porin gene of *Burkholderia* sp. NK8
764 involved in chemotaxis toward β-ketoadipate. *Biosci Biotechnol Biochem* 2015;79(6):926-36.

765 Yuan K, Xie X, Wang X *et al*. Transcriptional response of *Mycobacterium* sp. strain A1-PYR to
766 multiple polycyclic aromatic hydrocarbon contaminations. *Environ Pollut* 2018;243(Pt B):824-32.

767 **Figure legends**

768 **Fig. 1 Growth curves and aromatic compound degradation abilities of *C. necator***
769 **NH9.** Time course of bacterial growth (A) and aromatic compound degradation (B) of
770 strain NH9. Cells were grown on BSM supplemented with 5 mM 3-CB (circles), BA
771 (triangles), or CA (squares). Data are averages ± standard deviations of three independent
772 experiments. * and ** indicate significant differences at $p < 0.05$ and $p < 0.01$,
773 respectively (paired *t*-test). There was no significant difference in the OD_{600} values
774 between BA and CA samples at 12 h.

775 **Fig. 2 Transcript levels of genes involved in degradation of 3-CB and BA.** Boxes and
776 black circles indicate enzymes and compounds, respectively. TPM values of each gene are
777 average of triplicates and are shown in bar graphs. Scales of vertical axes of graph are
778 categorized into four groups with the following colors: blue, 10^5; orange, 10^4; purple, 10^3;
779 and gray, 10^2.

780 **Fig. 3 Evolutionary relationships among MFS transporters.** Construction of
781 evolutionary tree and ClustalW alignments were performed with MEGA version 7.0
782 (Kumar *et al*. 2016). Evolutionary relationships were inferred using the neighbor-joining
783 method (Saitou and Nei 1987). Red, blue, and green circles mark genes encoding MFS
784 transporters in NH9 expressed specifically in response to 3-CB, BA, and both compounds,
785 respectively. AAHS family includes BenK from *Acinetobacter baylyi* ADP1, BenK from
786 *Corynebacterium glutamicum* ATCC 13032, BenK from *Pseudomonas putida* CSV86,
787 BenP from *Cupriavidus pinatubonensis* JMP134, GalT from *P. putida* KTGAL, GenK
788 from *C. glutamicum* ATCC 13032, MhbT from *Klebsiella pneumoniae* M5a1, MhpT from
789 *Escherichia coli* K-12 substr. W3110, PcaK from *A. baylyi* ADP1, PcaK from *P. putida*
790 PRS2000, and TfdK from *C. pinatubonensis* JMP134. ACS family includes HpaX from *E.*

791 *coli* W and OphD from *Burkholderia multivorans* ATCC 17616. MHS family includes
792 CouT from *Rhodococcus jostii* RHA1, MopB from *Burkholderia cepacia* Pc701, and
793 PhdT from *C. glutamicum* ATCC 13032. See Table S4 for detailed information about
794 proteins.

795 **Fig. 4 GO enrichment analysis based on PAGE method.** Heat map colors represent
796 calculated Z-scores (FDR < 0.05) shown in figure. BP, biological process; CC, cellular
797 component; MF, molecular function.

798 **Fig. 5 Chemotaxis responses of *C. necator* NH9 in semi-solid agar plate assay.**
799 Chemotaxis of strain NH9 was tested in the presence of casamino acids (A), BA (B), 3-CB
800 (C) and BSM (D) for 3, 6, 14, and 14 h of incubation at 25°C, respectively. Arrows
801 indicate concentric rings, indicative of positive chemotaxis response. All experiments
802 were performed in triplicate.

803 **Fig. 6 Chemotaxis pathway model of *C. necator* NH9.** Detailed predicted chemotaxis
804 pathway of NH9 towards BA. See main text for descriptions of roles of genes encoding
805 MCPs (BJN34_09575, BJN34_21800, BJN34_24350, and BJN34_32190), CheA
806 (BJN34_21875), and CheY (BJN34_21830 and BJN34_21900). CheB (BJN34_21895),
807 CheD (BJN34_21890), and CheR (BJN34_21885) are involved in demethylation,
808 methylation, and deamidation of chemoreceptors, respectively. CheW (BJN34_21835 and
809 BJN34_21880) controls autophosphorylation activity of CheA. CheV (BJN34_33670)
810 functions as a coupling protein, similar to CheW, with additional phosphorylation
811 function. CheZ (BJN34_21905) can dephosphorylate CheY-P. Red arrows indicate genes
812 upregulated more than 2-fold (FDR < 0.05) by BA; blue arrows indicate genes
813 downregulated more than 2-fold (FDR < 0.05) by 3-CB. CCW and CW indicate
814 counterclockwise and clockwise, respectively. One MCP-encoding gene (BJN34_24350)

815 was upregulated by both BA and 3-CB. *cheW* (BJN34_21835) and *cheY* (BJN34_21900)
816 showed > 2-fold upregulation (FDR > 0.05) and < 2-fold upregulation, respectively.
817

818 **Graphical abstract caption**

819 RNA-seq analysis showed that 3-chlorobenzoate and benzoate induced the expression of
820 genes for aromatic degradation, transport, and/or chemotaxis strongly in *Cupriavidus*
821 *necator* NH9.

Table 1 Expression of genes involved in degradation of 3-chlorobenzoate and benzoate in NH9

Compound	Replicon	Locus	Gene[a]	K number	Definition[a]	3-CB vs. CA		BA vs. CA		3-CB vs. BA	
						LogFC[b]	FDR	LogFC[c]	FDR	LogFC[d]	FDR
3-Chlorobenzoate and Benzoate	Chr.1	BJN34_08560	*benA*	K05549	Benzoate 1,2-dioxygenase alpha subunit	8.2	1.2E-80	8.1	5.6E-79	0.092	9.0E-01
		BJN34_08565	*benB*	K05550	Benzoate 1,2-dioxygenase beta subunit	8.2	1.2E-91	8.0	5.1E-88	0.20	7.2E-01
		BJN34_08570	*benC*	K05784	Benzoate 1,2-dioxygenase reductase component	8.5	6.1E-140	8.3	4.9E-135	0.19	6.7E-01
		BJN34_08575	*benD*	K05783	1,6-Dihydroxycyclohexa-2,4-diene-1-carboxylate dehydrogenase	8.4	1.7E-117	8.4	4.4E-118	-0.048	9.4E-01
Benzoate	Chr.1	BJN34_07180	*boxA*	K15511	Benzoyl-CoA 2,3-epoxidase subunit A	1.3	2.8E-04	3.5	1.1E-25	-2.2	2.9E-12
		BJN34_07185	*boxB*	K15512	Benzoyl-CoA 2,3-epoxidase subunit B	1.1	9.9E-03	4.0	1.9E-23	-2.9	2.9E-14
		BJN34_07190	*boxC*	K15513	Benzoyl-CoA-dihydrodiol lyase	0.0052	9.9E-01	2.4	2.5E-05	-2.4	2.3E-05
		BJN34_07200	*bclA*	K04110	Benzoate-CoA ligase	0.67	4.8E-01	1.8	5.2E-02	-1.2	2.8E-01
	Chr.2	BJN34_32090	*boxA*	K15511	Benzoyl-CoA 2,3-epoxidase subunit A	0.56	3.3E-01	4.0	4.2E-23	-3.5	1.1E-19
		BJN34_32095	*boxB*	K15512	Benzoyl-CoA 2,3-epoxidase subunit B	0.51	3.5E-01	4.4	5.2E-24	-3.8	1.8E-20
		BJN34_32100	*boxC*	K15513	Benzoyl-CoA-dihydrodiol lyase	0.49	4.5E-01	3.8	3.2E-13	-3.3	6.5E-11
		BJN34_32115	*boxD*	K15514	3,4-Dehydroadipyl-CoA semialdehyde dehydrogenase	0.20	8.3E-01	4.9	6.9E-16	-4.7	2.0E-15
3-Chlorocatechol	pENH91	BJN34_37380	*cbnA*	K15253	Chlorocatechol 1,2-dioxygenase	9.9	7.5E-151	1.3	2.5E-05	8.6	2.5E-126
		BJN34_37385	*cbnB*	K01860	Chloromuconate cycloisomerase	9.8	2.2E-90	1.5	3.4E-04	8.3	2.0E-73
		BJN34_37395	*cbnC*	K01061	Dienelactone hydrolase	9.5	7.4E-148	1.4	3.1E-05	8.2	2.2E-123
		BJN34_37400	*cbnD*	K00217	Maleylacetate reductase	9.4	1.7E-122	1.5	2.9E-05	7.9	8.9E-100
Catechol	Chr.1	BJN34_08555	*catA*	K03381	Catechol 1,2-dioxygenase	6.0	5.8E-77	6.2	9.8E-80	-0.18	7.3E-01
	Chr.2	BJN34_24340	*catB*	K01856	Muconate cycloisomerase	5.6	2.9E-15	6.7	1.1E-19	-1.2	1.7E-01
		BJN34_29740	*catC*	K01055	3-Oxoadipate enol-lactonase	6.0	1.7E-67	6.0	8.8E-68	-0.044	9.5E-01
		BJN34_29745	*catD*	K03464	Muconolactone isomerase	5.9	7.7E-54	6.0	1.7E-54	-0.077	9.1E-01
3-Oxoadipate	Chr.2	BJN34_21015	*pcaI*	K01031	3-Oxoadipate CoA-transferase alpha subunit	4.5	2.9E-23	4.7	3.8E-24	-0.14	8.6E-01
		BJN34_21020	*pcaJ*	K01032	3-Oxoadipate CoA-transferase beta subunit	5.5	1.9E-28	5.3	2.7E-26	0.24	7.6E-01

BJN34_21025	*pcaF*	K00632	3-Oxoadipyl-CoA thiolase	5.9	1.8E-41	5.4	3.3E-36	0.48	4.1E-01

[a]Gene designations and definitions from KEGG annotation were manually modified.

[b]Log fold-change values calculated from 3-CB/CA.

[c]Log fold-change values calculated from BA/CA.

[d]Log fold-change values calculated from 3-CB/BA.

Table 2 Significantly expressed genes encoding MFS and ABC transporters in NH9

Family	Replicon	Locus	Component[a]	K number	Protein	Accession number	%Amino acid identity	3-CB vs. CA		BA vs. CA		3-CB vs. BA	
								LogFC[b]	FDR	LogFC[c]	FDR	LogFC[d]	FDR
Major facilitator superfamily (MFS)													
Aromatic acid:H^+ symporter (AAHS) family													
	Chr.1	BJN34_18155	-	K05548	BenP	AAZ63295.1	70.4	3.1	3.4E-20	0.12	8.9E-01	2.9	4.9E-20
	Chr.2	BJN34_30890	-	K08195	MhbT	AAW63412.1	52.1	4.2	1.3E-20	0.019	9.9E-01	4.1	2.6E-21
		BJN34_32125	-	K05548	BenP	AAZ63295.1	77.2	0.14	8.6E-01	4.5	4.4E-24	-4.3	3.8E-24
		BJN34_33870	-	K08195	PcaK	AAA85137.1	55.1	2.9	8.7E-09	1.3	2.0E-02	1.5	6.5E-03
Drug:H^+ antiporter-2 (14 spanner) (DHA2) family													
	Chr.1	BJN34_11715	-	K03446	PcaK	CAG68551.1	25.8	2.0	2.2E-07	1.8	1.5E-05	0.24	7.2E-01
		BJN34_12320	-	K19577	MhpT	APC50650.1	29.3	2.1	6.4E-11	-0.064	9.3E-01	2.1	1.3E-11
Metabolite:H^+ symporter (MHS) family													
	Chr.2	BJN34_20520	-	K03761	MopB	AAB41509.1	31.5	2.7	2.5E-10	2.1	1.7E-06	0.57	3.4E-01
Cyanate porter (CP) family													
	Chr.2	BJN34_26825	-	K03449	HpaX	ADT77978.1	26.8	2.9	1.4E-06	3.2	1.6E-07	-0.36	7.2E-01
ATP-binding cassette (ABC)													
Branched-chain amino acid transporter													
	Chr.1	BJN34_01710	NBD	K01995	HmgG	AAY18213.1	40.0	2.8	1.2E-11	2.1	5.0E-06	0.74	1.2E-01
		BJN34_01715	TMD	K01997	HmgE	AAY18215.1	28.3	2.7	5.5E-04	2.2	1.2E-02	0.46	6.9E-01
		BJN34_01720	TMD	K01998	HmgF	AAY18214.1	31.4	1.9	2.9E-05	1.5	4.3E-03	0.40	5.2E-01
		BJN34_01725	SBP	K01999	-	-	-	1.9	9.6E-09	1.4	1.5E-04	0.53	2.3E-01
		BJN34_01730	NBD	K01996	HmgH	AAY18212.1	44.3	2.1	3.0E-04	1.6	1.8E-02	0.49	5.6E-01

	BJN34_07675	SBP	K01999	-	-	-	1.8	1.2E-05	2.0	3.9E-06	-0.17	8.3E-01
	BJN34_07680	TMD	K01997	HmgE	AAY18215.1	24.6	0.51	3.2E-01	1.3	1.1E-02	-0.75	1.9E-01
	BJN34_07685	TMD	K01998	PcaV	CAC49878.1	24.9	0.91	4.9E-02	1.4	3.9E-03	-0.48	4.6E-01
	BJN34_07690	NBD	K01995	PcaW	CAC49877.1	34.3	0.062	9.7E-01	3.6	1.4E-03	-3.5	2.0E-03
	BJN34_07695	NBD	K01996	HmgH	AAY18212.1	40.7	1.0	2.4E-02	0.98	5.9E-02	0.030	9.8E-01
	BJN34_11495	TMD	K01998	PcaV	CAC49878.1	30.6	2.7	4.2E-13	2.1	7.3E-08	0.63	2.0E-01
	BJN34_11500	TMD	K01997	HmgE	AAY18215.1	29.5	3.0	9.7E-15	2.3	7.7E-09	0.72	1.6E-01
	BJN34_11505	NBD	K01996	HmgH	AAY18212.1	37.4	3.0	2.9E-18	2.4	2.4E-11	0.66	1.3E-01
	BJN34_11510	NBD	K01995	PcaW	CAC49877.1	40.2	0.72	3.6E-01	0.39	7.6E-01	0.34	7.7E-01
	BJN34_11515	SBP	K01999	PcaM	CAC49880.1	23.5	3.2	1.7E-17	2.3	1.5E-09	0.90	5.0E-02
Chr.2	BJN34_29445	SBP	K01999	PcaM	CAC49880.1	27.7	9.4	1.0E-89	1.5	3.8E-02	7.9	6.9E-80
	BJN34_29450	NBD	K01995	PcaW	CAC49877.1	35.8	11.0	2.3E-85	3.8	1.4E-05	7.3	1.8E-67
	BJN34_29455	NBD	K01996	PcaX	CAC49876.1	40.3	8.9	5.3E-91	0.91	3.8E-01	8.0	4.4E-88
	BJN34_29460	TMD	K01997	PcaN	CAC49879.1	33.3	8.1	3.8E-05	1.5	5.6E-01	6.6	1.1E-03
	BJN34_29465	TMD	K01998	PcaV	CAC49878.1	32.4	7.7	2.5E-27	0.47	7.3E-01	7.2	8.9E-26
	BJN34_32550	TMD	K01997	HmgE	AAY18215.1	38.5	0.56	2.3E-01	0.55	3.4E-01	0.0051	1.0E+00
	BJN34_32555	TMD	K01998	HmgF	AAY18214.1	27.3	2.5	5.4E-06	2.2	2.7E-04	0.30	7.0E-01
	BJN34_32560	NBD	K01995	HmgG	AAY18213.1	41.9	1.3	1.4E-02	1.5	4.6E-03	-0.27	7.2E-01
	BJN34_32565	NBD	K01996	HmgH	AAY18212.1	45.5	2.5	1.0E-04	2.2	2.2E-03	0.29	7.4E-01
	BJN34_32570	SBP	K01999	HmgD	AAY18216.1	28.4	1.6	1.1E-06	1.0	7.0E-03	0.57	1.8E-01
NitT/TauT family transporter												
Chr.1	BJN34_09335	SBP	K02051	-	-	-	1.3	2.9E-02	0.40	7.0E-01	0.89	2.3E-01
	BJN34_09340	NBD	K02049	PatA	ABG99217.1	41.4	2.3	5.1E-06	0.82	3.4E-01	1.5	3.1E-03
	BJN34_09345	TMD	K02050	PatC	ABG99215.1	27.0	2.2	8.8E-04	1.2	2.0E-01	1.0	1.9E-01

	BJN34_36080	SBP	K02051	-	-	-	1.2	1.9E-01	-1.2	3.9E-01	2.4	2.5E-02
pENH92	BJN34_36095	TMD	K02050	PatB	ABG99216.1	26.9	2.5	4.6E-04	-0.018	9.9E-01	2.5	7.9E-04
	BJN34_36100	NBD	K02049	PatA	ABG99217.1	44.1	2.9	3.5E-04	1.8	1.2E-01	1.2	1.8E-01
Glycerol transporter												
	BJN34_13400	SBP	K17321	-	-	-	2.3	4.3E-09	1.4	2.3E-03	0.97	4.3E-02
	BJN34_13410	TMD	K17323	-	-	-	2.0	2.3E-05	1.6	2.2E-03	0.35	5.8E-01
Chr.1	BJN34_13415	TMD	K17322	-	-	-	1.6	1.5E-03	1.6	3.3E-03	-0.0088	9.9E-01
	BJN34_13420	NBD	K17325	OphH	BAG45601.1	34.9	2.2	1.3E-02	1.4	1.9E-01	0.74	5.7E-01
	BJN34_13425	NBD	K17324	PatA	ABG99217.1	30.3	1.2	7.3E-04	1.1	6.2E-03	0.11	8.6E-01
Putative polar amino acid transporter												
	BJN34_14830	TMD	K02029	-	-	-	2.7	4.9E-07	-0.40	7.2E-01	3.1	1.5E-08
Chr.1	BJN34_14835	TMD	K02029	-	-	-	3.7	1.1E-05	1.2	3.1E-01	2.5	5.4E-03
	BJN34_14840	NBD	K02028	OphH	BAG45601.1	35.3	2.7	1.6E-10	1.1	5.6E-02	1.7	1.1E-04
	BJN34_14845	SBP	K02030	-	-	-	2.0	9.1E-07	0.70	2.2E-01	1.3	3.7E-03
ABC-2 type transporter												
Chr.2	BJN34_25255	NBD	K01990	OphH	BAG45601.1	31.9	3.5	1.7E-02	2.3	2.5E-01	1.1	4.9E-01
	BJN34_25270	TMD	K01992	-	-	-	4.8	1.2E-02	4.7	3.5E-02	0.14	9.5E-01
Ribose transporter												
	BJN34_29355	NBD	K10441	HmgG	AAY18213.1	28.3	2.6	1.3E-11	2.0	6.6E-07	0.61	2.4E-01
Chr.2	BJN34_29360	TMD	K10440	HmgE	AAY18215.1	26.0	2.6	2.6E-08	2.4	5.0E-07	0.17	8.4E-01
	BJN34_29365	SBP	K10439	-	-	-	2.5	6.2E-10	2.6	3.0E-10	-0.077	9.2E-01
Other ABC transporters												
Chr.1	BJN34_11055	NBD, TMD	K02471	HmgG	AAY18213.1	38.0	2.4	1.1E-02	1.6	2.0E-01	0.85	5.2E-01

[a]NBD, nucleotide binding domain; SBP, substrate binding protein; TMD, transmembrane domain.

[b]Log fold-change values calculated from 3-CB/CA.

[c]Log fold-change values calculated from BA/CA.

[d]Log fold-change values calculated from 3-CB/BA.

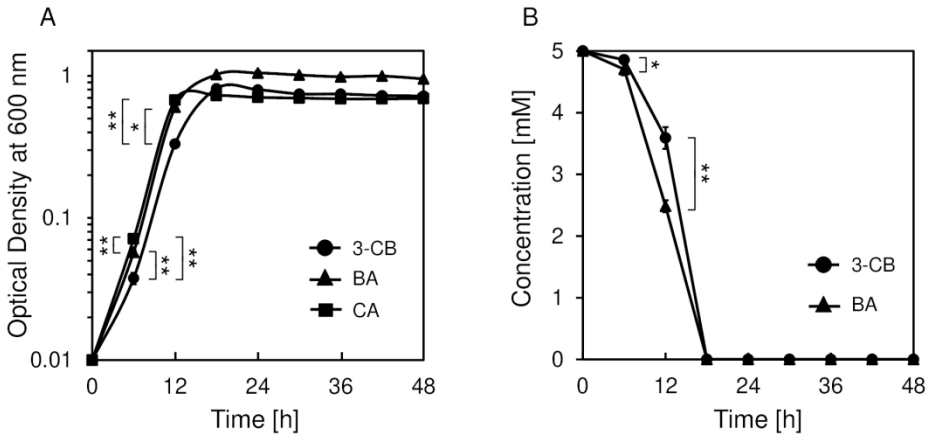

Fig. 1 Growth curves and aromatic compound degradation abilities of *C. necator* NH9. Time course of bacterial growth (A) and aromatic compound degradation (B) of strain NH9. Cells were grown on BSM supplemented with 5 mM 3-CB (circles), BA (triangles), or CA (squares). Data are averages ± standard deviations of three independent experiments. * and ** indicate significant differences at $p < 0.05$ and $p < 0.01$, respectively (paired t-test). There was no significant difference in the OD_{600} values between BA and CA samples at 12 h.

254x190mm (200 x 200 DPI)

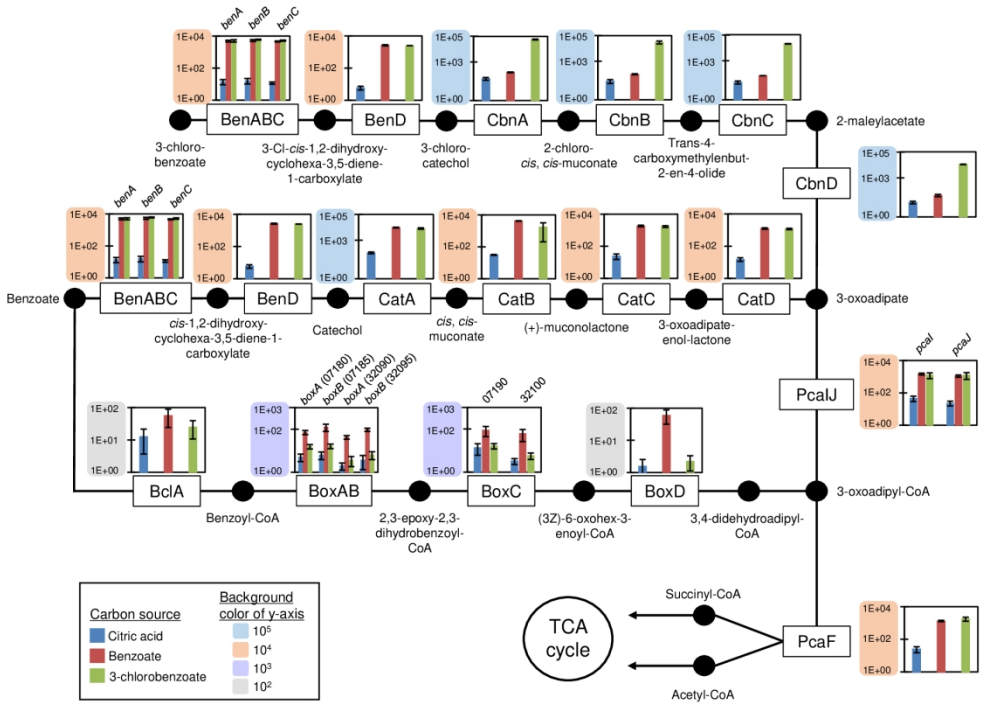

Fig. 2 Transcript levels of genes involved in degradation of 3-CB and BA. Boxes and black circles indicate enzymes and compounds, respectively. TPM values of each gene are average of triplicates and are shown in bar graphs. Scales of vertical axes of graph are categorized into four groups with the following colors: blue, 10^5; orange, 10^4; purple, 10^3; and gray, 10^2.

254x190mm (200 x 200 DPI)

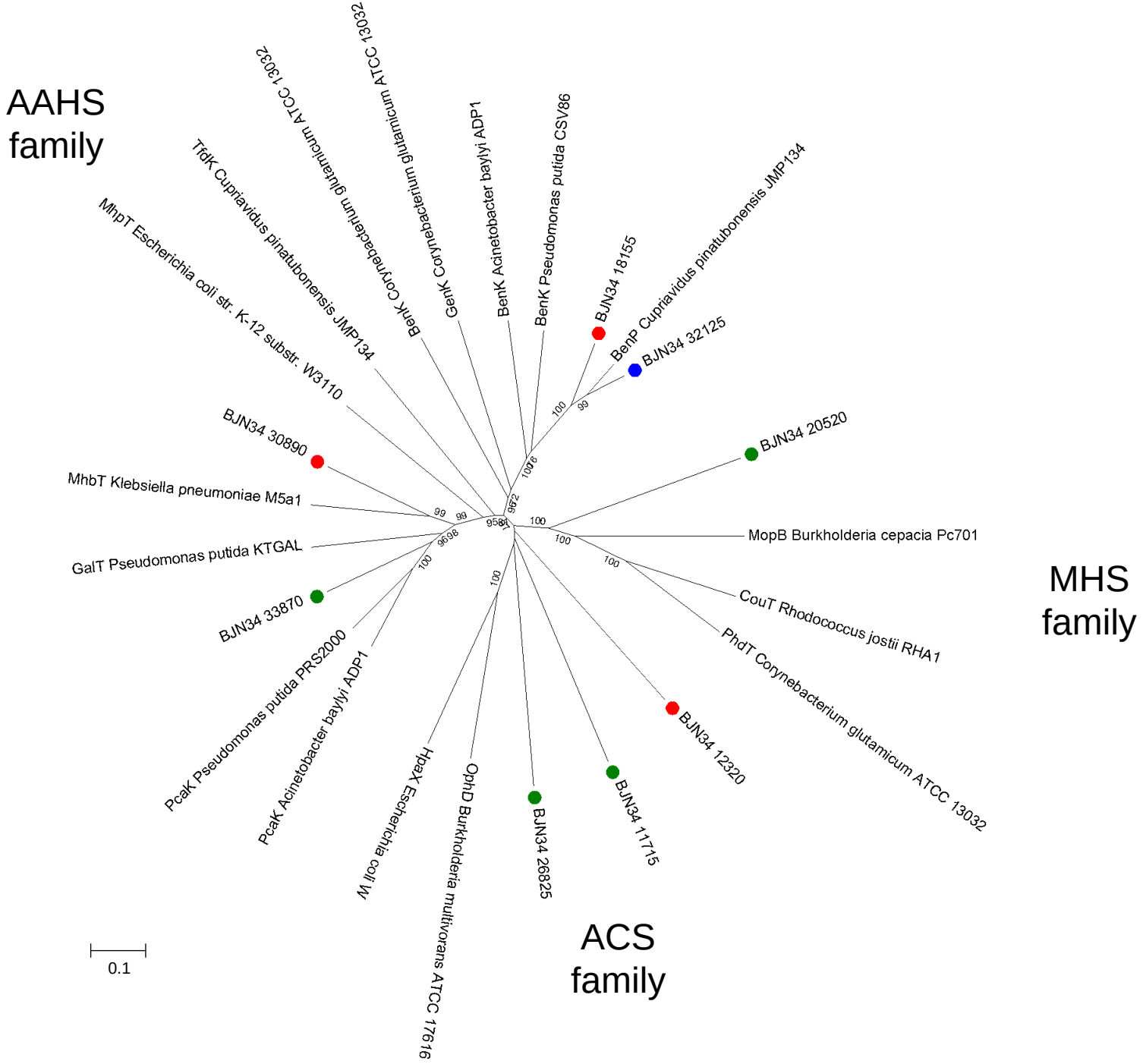
AAHS family
MHS family
ACS family
TfdK Cupriavidus pinatubonensis JMP134
MhpT Escherichia coli str. K-12 substr. W3110
BJN34 30890
MhbT Klebsiella pneumoniae M5a1
GalT Pseudomonas putida KTGAL
BJN34 33870
PcaK Pseudomonas putida PRS2000
PcaK Acinetobacter baylyi ADP1
HpaX Escherichia coli W
OphD Burkholderia multivorans ATCC 17616
BJN34 26825
BJN34 11715
BJN34 12320
PhdT Corynebacterium glutamicum ATCC 13032
CouT Rhodococcus jostii RHA1
MopB Burkholderia cepacia Pc701
BJN34 20520
BJN34 32125
BenP Cupriavidus pinatubonensis JMP134
BJN34 18155
BenK Pseudomonas putida CSV86
BenK Acinetobacter baylyi ADP1
GenK Corynebacterium glutamicum ATCC 13032
BenK Corynebacterium glutamicum ATCC 13032
0.1

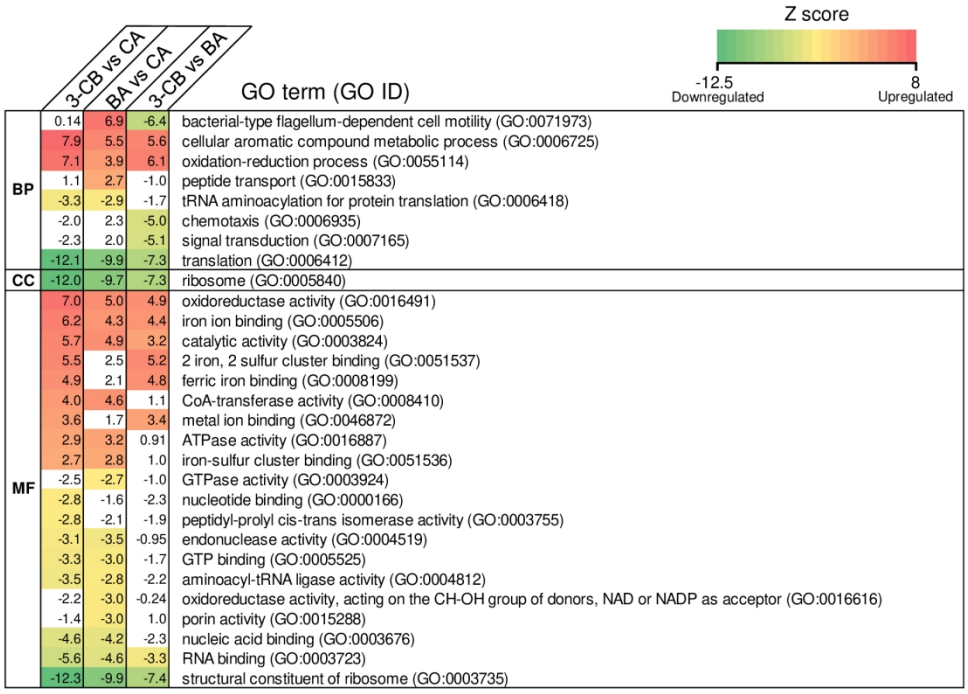

Fig. 4 GO enrichment analysis based on PAGE method. Heat map colors represent calculated Z-scores (FDR < 0.05) shown in figure. BP, biological process; CC, cellular component; MF, molecular function.

254x190mm (200 x 200 DPI)

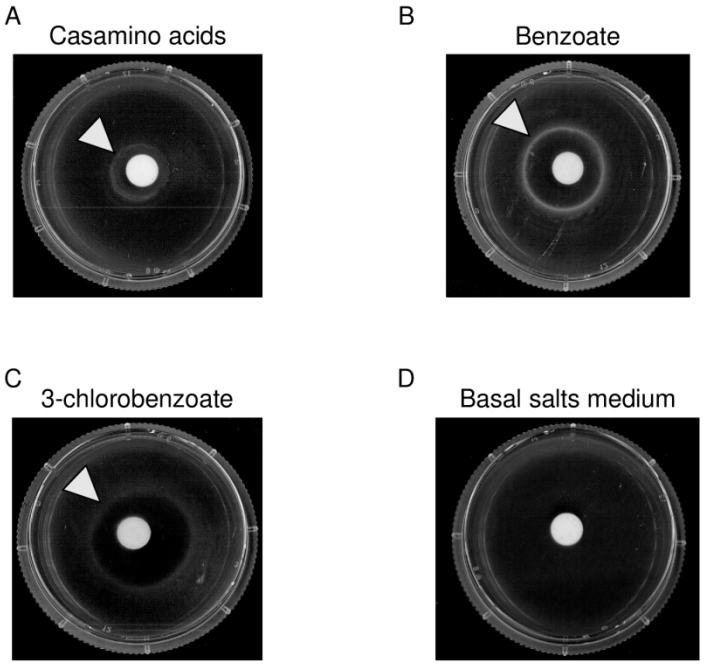

Fig. 5 Chemotaxis responses of *C. necator* NH9 in semi-solid agar plate assay. Chemotaxis of strain NH9 was tested in the presence of casamino acids (A), BA (B), 3-CB (C) and BSM (D) for 3, 6, 14, and 14 h of incubation at 25°C, respectively. Arrows indicate concentric rings, indicative of positive chemotaxis response. All experiments were performed in triplicate.

254x190mm (200 x 200 DPI)

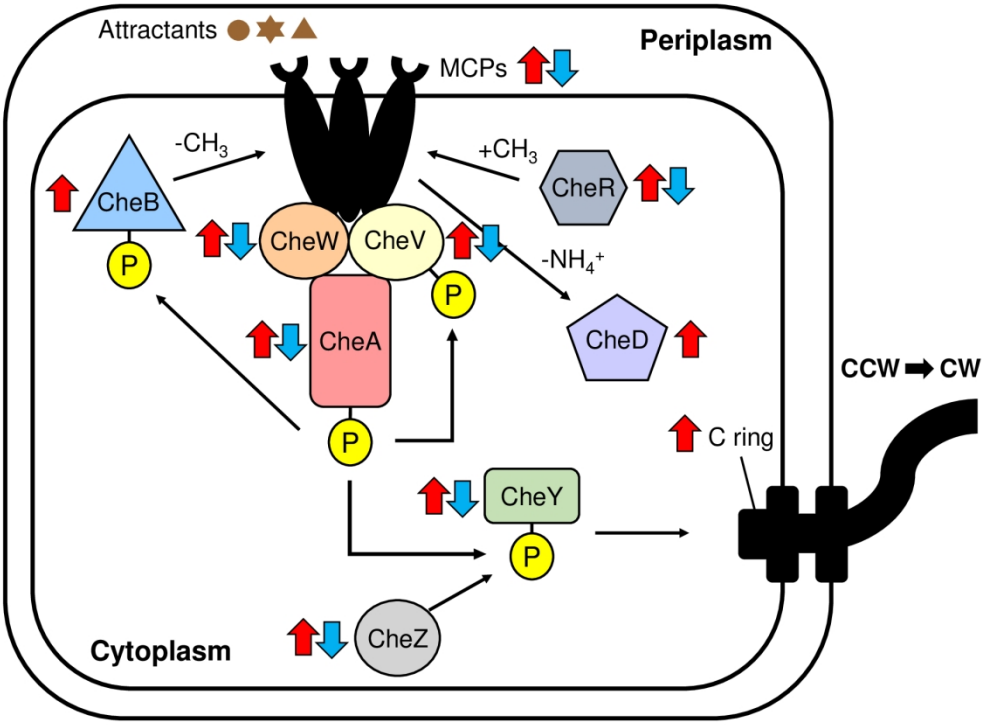

Fig. 6 Chemotaxis pathway model of *C. necator* NH9. Detailed predicted chemotaxis pathway of NH9 towards BA. See main text for descriptions of roles of genes encoding MCPs (BJN34_09575, BJN34_21800, BJN34_24350, and BJN34_32190), CheA (BJN34_21875), and CheY (BJN34_21830 and BJN34_21900). CheB (BJN34_21895), CheD (BJN34_21890), and CheR (BJN34_21885) are involved in demethylation, methylation, and deamidation of chemoreceptors, respectively. CheW (BJN34_21835 and BJN34_21880) controls autophosphorylation activity of CheA. CheV (BJN34_33670) functions as a coupling protein, similar to CheW, with additional phosphorylation function. CheZ (BJN34_21905) can dephosphorylate CheY-P. Red arrows indicate genes upregulated more than 2-fold (FDR < 0.05) by BA; blue arrows indicate genes downregulated more than 2-fold (FDR < 0.05) by 3-CB. CCW and CW indicate counterclockwise and clockwise, respectively. One MCP-encoding gene (BJN34_24350) was upregulated by both BA and 3-CB. *cheW* (BJN34_21835) and *cheY* (BJN34_21900) showed > 2-fold upregulation (FDR > 0.05) and < 2-fold upregulation, respectively.

254x190mm (200 x 200 DPI)

Supplementary Material

Transcriptome differences between *Cupriavidus necator* NH9 grown with 3-chlorobenzoate and that grown with benzoate

Ryota Moriuchi[1,2], Hideo Dohra[1], Yu Kanesaki[1] and Naoto Ogawa[2,3*]

[1]Research Institute of Green Science and Technology, Shizuoka University, 836 Ohya, Suruga-ku, Shizuoka-shi, Shizuoka 422-8529, Japan

[2]The United Graduate School of Agricultural Science, Gifu University, 1-1 Yanagido, Gifu-shi, Gifu 501-1193, Japan

[3]Graduate School of Integrated Science and Technology, Shizuoka University, 836 Ohya, Suruga-ku, Shizuoka-shi, Shizuoka 422-8529, Japan

Correspondence:

Naoto Ogawa

Faculty of Agriculture, Shizuoka University,

836 Ohya, Suruga-ku, Shizuoka-shi, Shizuoka, 422-8529, Japan.

E-mail address: ogawa.naoto@shizuoka.ac.jp

Tel/Fax: +81-54-238-4875/+81-54-237-3028

The Supplementary Material includes:

- Figures S1-S4
- Tables S1-S7
- References (Figure S4 and Table S4)

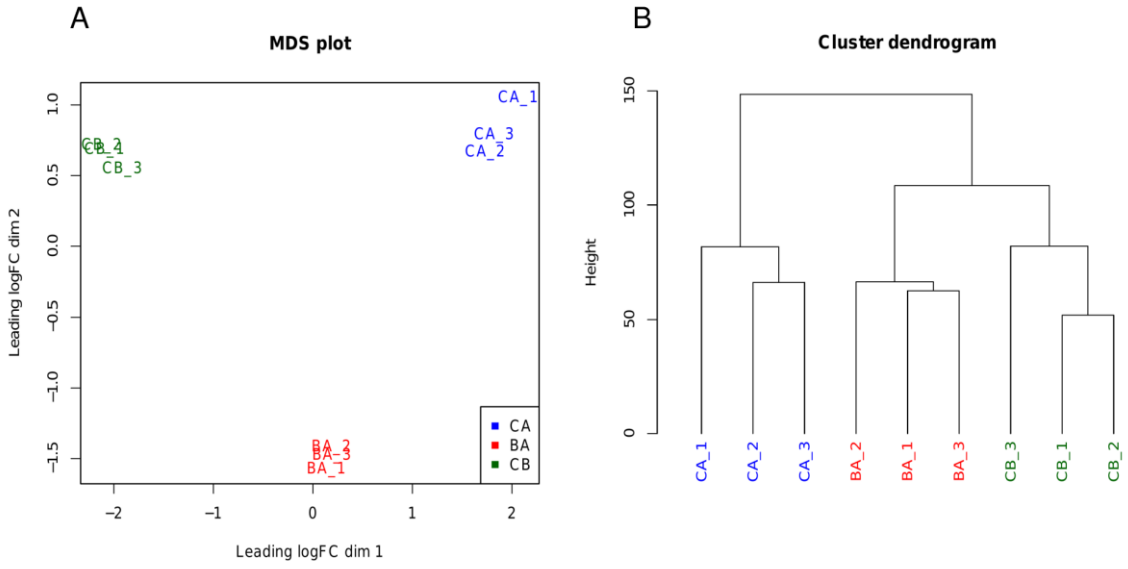

Figure S1. Assessment for correlation of gene expression profiling.
Multi-dimensional scaling plot for read counts data (A). Cluster dendrogram for log2 counts per million mapped reads (B). BA, benzoate; CA, citric acid; CB, 3-chlorobenzoate.

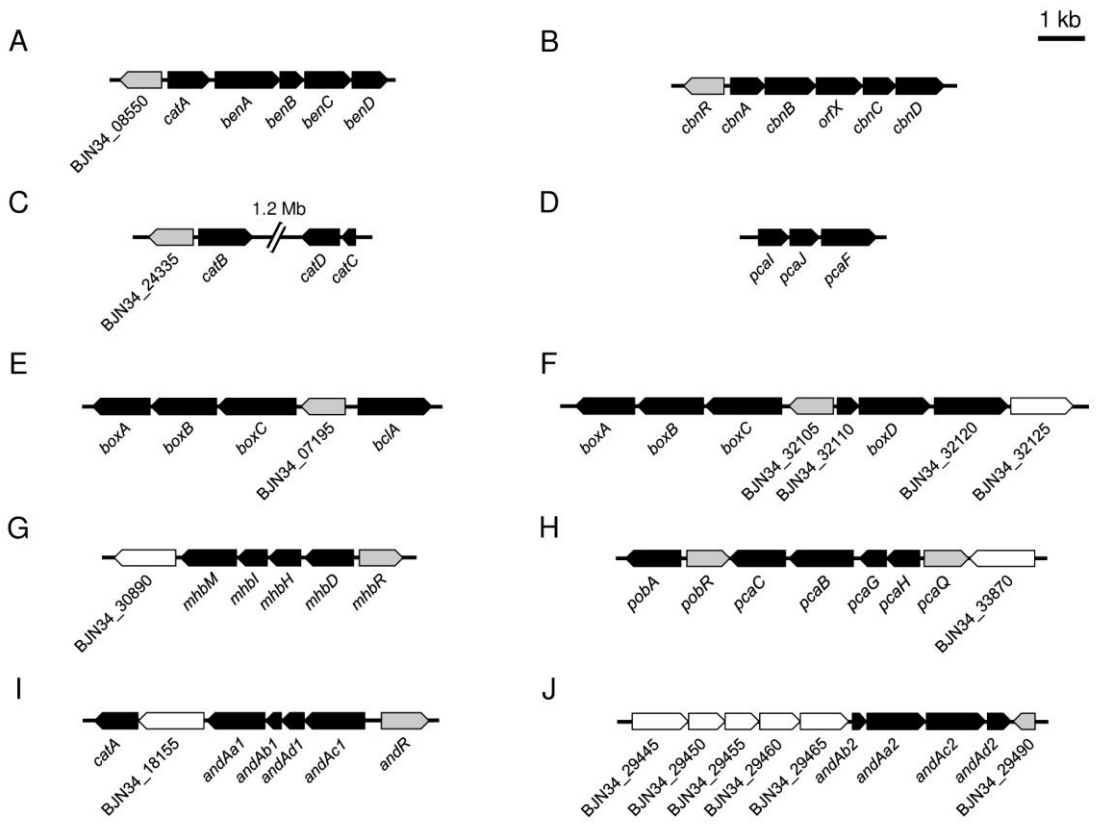

Figure S2. Arrangement of genes involved in degradation and transport of aromatic compounds in the *C. necator* NH9 genome.

ben and *catA* on chromosome 1. BJN34_08550 encodes LysR-type transcriptional regulator (A). *cbn* on pENH91 (B). *cat* on chromosome 2. BJN34_24335 encodes a LysR-type transcriptional regulator (C). *pca* on chromosome 2 (D). *boxABC* and *bclA* on chromosome 1. BJN34_07195 encodes helix-turn-helix transcriptional regulator (E). *boxABCD* genes on chromosome 2. BJN34_32105, BJN34_32110, BJN34_32120 and BJN34_32125 encode a helix-turn-helix transcriptional regulator, a DUF4863 domain-containing protein, a benzoate-CoA ligase family protein, and an MFS transporter, respectively (F). *mhb* on chromosome 2. BJN34_30890 encodes an MFS transporter (G). *pob* and *pca* on chromosome 2. BJN34_33870 encodes an MFS transporter (H). *and1* on chromosome 1. BJN34_18155 encodes an MFS transporter (I). *and2* on chromosome 2. BJN34_29445 to BJN34_29465 encode components of ABC-type transporter. BJN34_29490 encodes a MarR family transcriptional regulator (J). Genes encoding transcriptional regulators, transporters, and other functions are colored in gray, white, and black, respectively.

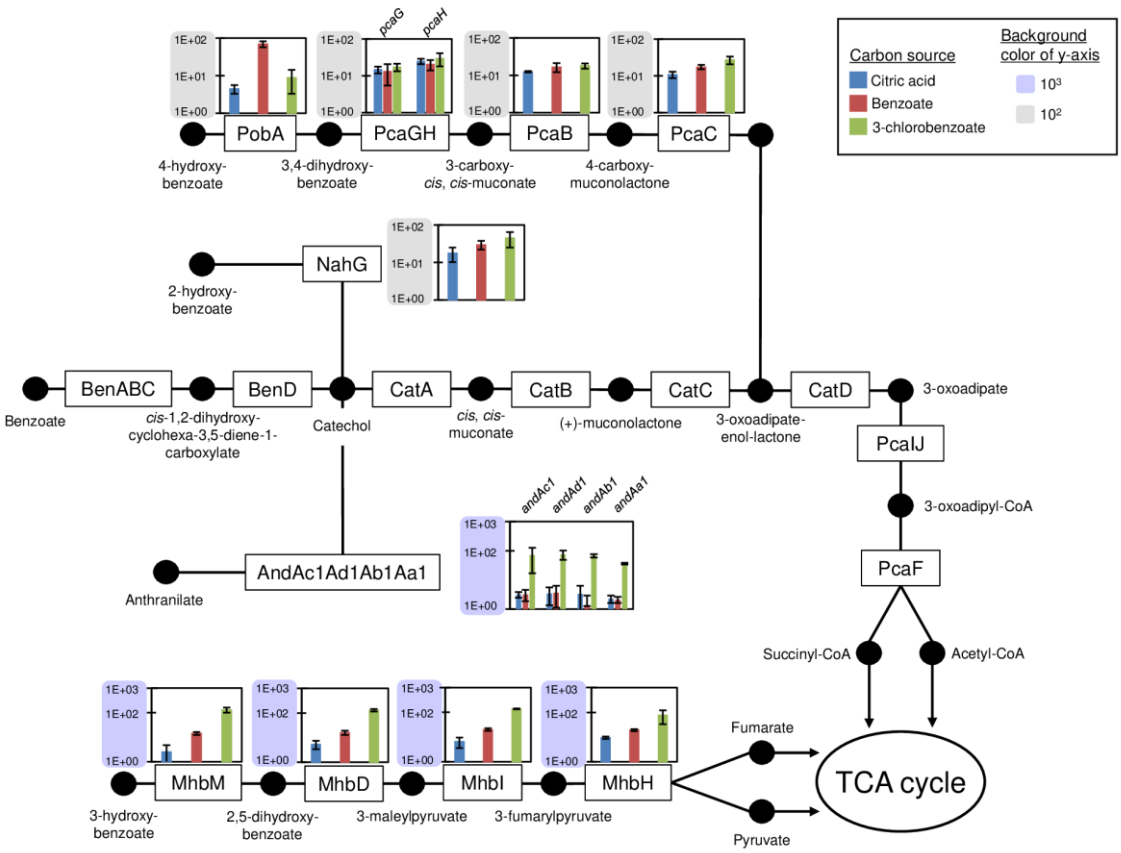

Figure S3. Expression of genes involved in degradation of hydroxybenzoate and anthranilate.

Boxes and black circles indicate enzymes and compounds, respectively. TPM values of each gene are average of triplicates and are shown as bar graphs. Scales of vertical axes of graph are categorized into two groups with the following colors: purple, 10^3; and gray, 10^2. Bar graphs of *benABCD*, *catABCD* and *pcaIJF* genes are shown in Fig. 2.

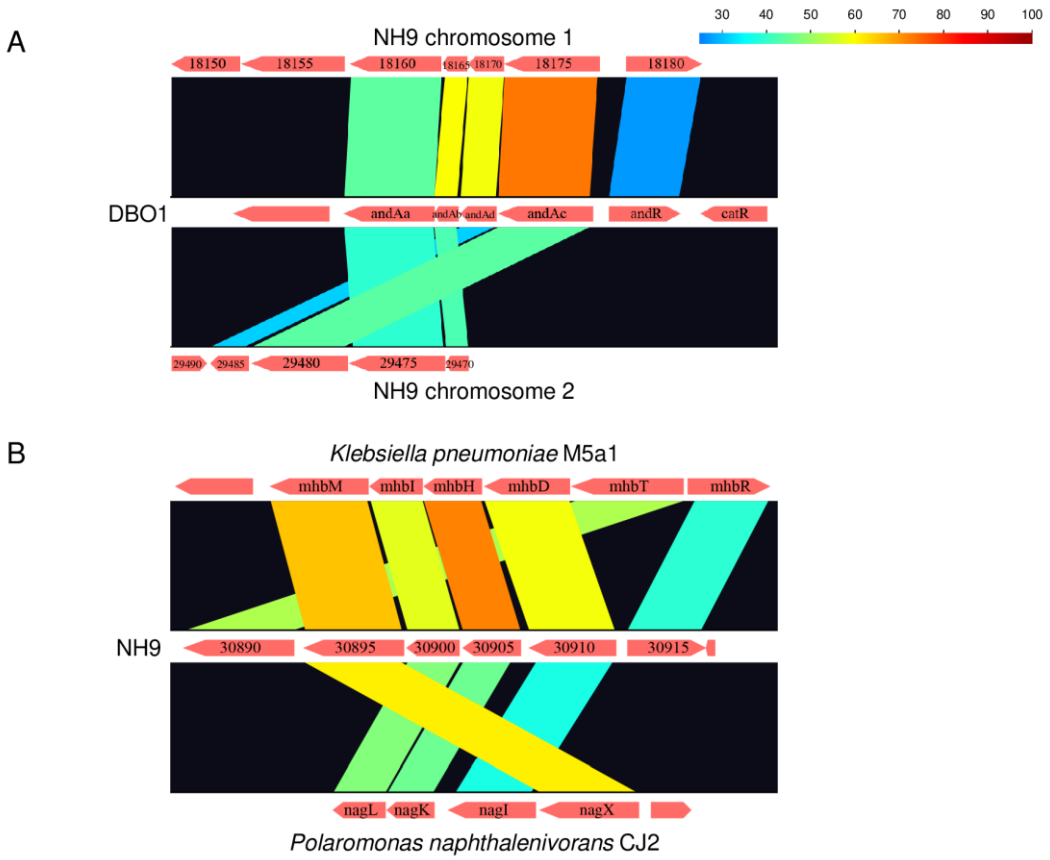

Figure S4. Parallel view of And (A) and Mhb (B) proteins.

Linear comparison of And protein sequences derived from *Burkholderia cepacia* DBO1 (AY223539) and *Cupriavidus necator* NH9 (CP017757 and CP017758), and of Mhb protein sequences derived from *Klebsiella pneumoniae* M5a1 (AY648560), *C. necator* NH9 (CP017758), and *Polaromonas naphthalenivorans* CJ2 (DQ167475). Numerical numbers indicate the numbers of locus tag of the genes in strain NH9. These protein sequence comparisons were performed by GenomeMatcher (Ohtsubo *et al*. 2008).

Reference (Figure S4)

Ohtsubo Y, Ikeda-Ohtsubo W, Nagata Y *et al*. GenomeMatcher: a graphical user interface for DNA sequence comparison. *BMC Bioinformatics* 2008;9:376.

Table S1 Information of RNA-seq in this study

Substrate	Replicate	Total numbers of raw reads[a]	Total numbers of filtered reads[a]	Total bases of filtered reads[a] (bp)	Average read coverage[b]	Total numbers of mapped reads[a]	Total numbers of rRNA reads[a]	Accession number
3-Chlorobenzoate	1	4,470,112	4,396,122	328,961,687	39.9	4,366,446 (99.3%)	196,339 (4.5%)	DRR232377
	2	4,477,266	4,409,332	329,953,800	40.0	4,381,299 (99.4%)	161,452 (3.7%)	DRR232378
	3	4,587,986	4,519,530	338,284,464	41.0	4,483,673 (99.2%)	109,326 (2.4%)	DRR232379
Benzoate	1	4,726,910	4,657,486	348,453,632	42.3	4,622,278 (99.2%)	181,549 (3.9%)	DRR232380
	2	4,494,100	4,435,928	332,010,152	40.3	4,407,455 (99.4%)	65,971 (1.5%)	DRR232381
	3	4,533,626	4,450,798	333,099,568	40.4	4,412,173 (99.1%)	97,939 (2.2%)	DRR232382
Citric acid	1	4,278,198	4,215,380	315,422,818	38.2	4,179,859 (99.2%)	103,433 (2.5%)	DRR232374
	2	4,469,226	4,393,456	328,723,313	39.9	4,341,530 (98.8%)	157,478 (3.6%)	DRR232375
	3	4,240,250	4,172,854	312,306,760	37.9	4,141,094 (99.2%)	68,860 (1.7%)	DRR232376

[a]Paired-end reads.

[b]Calculated from total bases of filtered reads (bp) / genome size of strain NH9 (8,246,935 bp).

Table S2 Expression of genes involved in degradation of hydroxybenzoate and anthranilate in NH9

Compound	Replicon	Locus	Gene[a]	K number	Definition[a]	3-CB vs. CA		BA vs. CA		3-CB vs. BA	
						LogFC[b]	FDR	LogFC[c]	FDR	LogFC[d]	FDR
2-Hydroxybenzoate	Chr.2	BJN34_24950	*nahG*	K00480	Salicylate hydroxylase	1.1	3.3E-02	0.42	6.0E-01	0.67	3.3E-01
3-Hydroxybenzoate	Chr.2	BJN34_30895	*mhbM*[e]	K22270	3-Hydroxybenzoate 6-monooxygenase	5.3	3.5E-14	2.1	6.1E-03	3.2	1.1E-06
		BJN34_30900[a]	*mhbI*[e]	K01801	Maleylpyruvate isomerase	4.2	9.9E-39	1.2	8.2E-03	3.1	8.9E-26
		BJN34_30905	*mhbH*[e]	K16165	Fumarylpyruvate hydrolase	4.1	1.5E-34	1.3	1.8E-03	2.8	3.2E-20
		BJN34_30910	*mhbD*[e]	K00450	Gentisate 1,2-dioxygenase	2.8	1.8E-08	0.70	3.2E-01	2.1	4.9E-05
4-Hydroxybenzoate	Chr.2	BJN34_33835	*pobA*	K00481	4-Hydroxybenzoate 3-monooxygenase	0.75	2.1E-01	3.6	5.2E-12	-2.9	2.0E-08
		BJN34_33845	*pcaC*[e]	K01607[e]	4-Carboxymuconolactone decarboxylase	0.99	1.5E-03	0.34	4.9E-01	0.65	8.6E-02
		BJN34_33850	*pcaB*	K01857	3-Carboxy-*cis*,*cis*-muconate cycloisomerase	0.24	5.9E-01	0.089	9.0E-01	0.15	8.2E-01
		BJN34_33855	*pcaG*	K00448	Protocatechuate 3,4-dioxygenase alpha subunit	-0.060	9.3E-01	-0.51	5.1E-01	0.45	5.7E-01
		BJN34_33860	*pcaH*	K00449	Protocatechuate 3,4-dioxygenase beta subunit	-0.043	9.4E-01	-0.62	2.8E-01	0.58	3.3E-01
Anthranilate	Chr.1	BJN34_18160	*andAa1*	K00529	Anthranilate 1,2-dioxygenase ferredoxin reductase component	3.7	3.5E-26	-0.44	5.7E-01	4.1	8.4E-32
		BJN34_18165	*andAb1*	K18248	Anthranilate 1,2-dioxygenase ferredoxin component	3.9	1.2E-10	-1.6	1.6E-01	5.4	4.4E-16
		BJN34_18170	*andAd1*	K16320	Anthranilate 1,2-dioxygenase small subunit	4.1	6.5E-10	-0.23	8.8E-01	4.3	9.0E-11

BJN34_18175	*andAc1*	K16319	Anthranilate 1,2-dioxygenase large subunit	4.3	5.1E-10	-0.32	8.1E-01	4.6	5.0E-11

[a]Gene designation and definition from KEGG annotation were manually modified.

[b]Log fold-change values calculated from 3-CB/CA.

[c]Log fold-change values calculated from BA/CA.

[d]Log fold-change values calculated from 3-CB/BA.

[e]Changed from previous study, Moriuchi *et al*., 2019.

Table S3 Expression of other characteristic genes

Replicon	Locus	Gene[a]	K number	Description	3-CB vs. CA		BA vs. CA		3-CB vs. BA	
					LogFC[b]	FDR	LogFC[c]	FDR	LogFC[d]	FDR
Putative anthranilate degradation genes										
Chr.2	BJN34_29470	*andAb2*	K05710	3-Phenylpropionate/trans-cinnamate dioxygenase ferredoxin component[e]	8.0	2.0E-20	1.4	2.2E-01	6.5	1.5E-16
	BJN34_29475	*andAa2*	K00529	3-Phenylpropionate/trans-cinnamate dioxygenase ferredoxin reductase component[e]	8.9	6.4E-44	2.2	3.9E-03	6.7	2.5E-33
	BJN34_29480	*andAc2*	K16319	Anthranilate 1,2-dioxygenase large subunit[e]	8.3	2.0E-81	1.5	9.9E-04	6.8	4.3E-65
	BJN34_29485	*andAd2*	K16320	Anthranilate 1,2-dioxygenase small subunit[e]	7.9	8.8E-47	0.96	1.7E-01	6.9	1.6E-40
Stress response genes										
Chr.1	BJN34_00915	*hslV*	K01419	HslU--HslV peptidase proteolytic subunit	1.1	9.8E-02	1.8	6.8E-03	-0.76	3.8E-01
	BJN34_00920	*hslU*	K03667	HslU--HslV peptidase ATPase subunit	1.2	1.4E-01	2.0	1.9E-02	-0.80	4.6E-01
	BJN34_04025	*groES*	K04078	chaperonin GroES[e]	0.78	9.8E-02	0.47	4.7E-01	0.30	6.8E-01
	BJN34_04030	*groEL*	K04077	chaperonin GroEL[e]	0.85	6.1E-02	0.47	4.7E-01	0.38	5.8E-01
	BJN34_06000	*grpE*	K03687	molecular chaperone GrpE[e]	0.85	1.6E-01	1.7	7.8E-03	-0.81	2.9E-01
	BJN34_07555	*clpP*	K01358	ATP-dependent Clp endopeptidase, proteolytic subunit ClpP	-0.68	1.5E-02	-0.56	9.1E-02	-0.11	8.2E-01
	BJN34_07560	*clpX*	K03544	ATP-dependent protease ATP-binding subunit ClpX	-0.031	9.3E-01	-0.36	3.0E-01	0.33	3.7E-01
	BJN34_09490	*dnaK*	K04043	molecular chaperone DnaK	1.8	4.4E-04	2.0	1.6E-04	-0.24	7.9E-01
	BJN34_09495	*groEL*	K04077	chaperonin GroEL[e]	1.4	2.7E-03	1.8	3.3E-04	-0.37	6.2E-01
	BJN34_09500	*groES*	K04078	chaperonin GroES[e]	1.8	5.7E-03	2.1	3.9E-03	-0.25	8.3E-01
	BJN34_11475	*clpB*	K03695	ATP-dependent chaperone ClpB	1.5	2.1E-02	2.2	1.8E-03	-0.68	4.9E-01
	BJN34_16310	*clpA*	K03694	ATP-dependent Clp protease ATP-binding subunit ClpA	0.68	7.2E-02	0.60	1.9E-01	0.074	9.2E-01

	BJN34_16495	*dnaJ*	K03686	molecular chaperone DnaJ	-0.18	7.4E-01	0.79	1.2E-01	-0.97	5.2E-02
	BJN34_16500	*dnaK*	K04043	molecular chaperone DnaK	0.54	4.2E-01	1.5	2.4E-02	-0.94	2.2E-01
Benzoate stress response genes										
Chr.1	BJN34_02220	*cyoE*	K02257	protoheme IX farnesyltransferase	-0.98	5.4E-03	-0.39	4.4E-01	-0.58	2.1E-01
	BJN34_03315	*sucC*	K01903	succinyl-CoA synthetase beta subunit[e]	-1.4	3.6E-05	-1.3	7.5E-04	-0.16	8.0E-01
	BJN34_03320	*sucD*	K01902	succinyl-CoA synthetase alpha subunit[e]	-1.4	2.9E-05	-1.4	9.4E-05	-0.015	9.9E-01
	BJN34_13095	*pstB*	K02036	phosphate ABC transporter ATP-binding protein	1.2	7.6E-03	0.15	8.7E-01	1.1	4.9E-02
	BJN34_13100	*pstA*	K02038	phosphate ABC transporter, permease protein PstA	1.4	3.2E-02	-0.26	8.4E-01	1.6	2.6E-02
	BJN34_13105	*pstC*	K02037	phosphate ABC transporter permease subunit PstC	1.5	1.0E-02	-0.50	6.0E-01	2.0	1.6E-03
	BJN34_13110	*pstS*	K02040	phosphate ABC transporter substrate-binding protein PstS	1.4	4.1E-05	-0.43	4.1E-01	1.9	1.4E-07
	BJN34_15890	*btuB*	K16092	TonB-dependent receptor	-1.3	2.0E-03	-0.72	1.7E-01	-0.54	3.5E-01
	BJN34_16665	*cybB*	K12262	superoxide oxidase[e]	-0.20	6.0E-01	1.9	1.2E-10	-2.1	5.7E-13
	BJN34_16755	*bamE*	K06186	outer membrane protein assembly factor BamE	-1.5	3.4E-05	-0.53	2.8E-01	-0.96	2.7E-02
Chr.2	BJN34_23155	*kdpD*	K07646	two-component system, OmpR family, sensor histidine kinase KdpD[e]	-0.24	8.6E-01	-0.53	7.7E-01	0.29	8.8E-01
	BJN34_25760	*lpxL*	K02517	lipid A biosynthesis lauroyl acyltransferase	-1.0	9.8E-02	-0.14	9.0E-01	-0.86	2.7E-01
Polyhydroxybutyrate synthesis genes										
Chr.1	BJN34_07300	*phaC*	K03821	polyhydroxyalkanoate synthase subunit PhaC[e]	0.63	9.1E-02	0.39	4.6E-01	0.24	6.8E-01
	BJN34_07305	*phaA*	K00626	acetyl-CoA acetyltransferase	0.77	6.5E-02	0.68	1.8E-01	0.088	9.1E-01
	BJN34_07310	*phaB*	K00023	acetoacetyl-CoA reductase[e]	1.2	1.7E-03	0.86	5.6E-02	0.33	5.9E-01
	BJN34_07315	*phaR*	-	polyhydroxyalkanoate synthesis repressor PhaR	0.13	7.3E-01	-0.32	4.5E-01	0.44	2.4E-01

[a]Gene designation from KEGG annotation were manually modified.

[b]Log fold-change values calculated from 3-CB/CA.

[c]Log fold-change values calculated from BA/CA.

[d]Log fold-change values calculated from 3-CB/BA.

[e]KEGG definition.

Table S4 Aromatic compound transporters that have been experimentally verified or examined for their functions

Family	Protein	Accession number	Component[a]	Strain	Substrate or putative substrate	Reference
Major facilitator superfamily (MFS)						
Aromatic acid:H^+ symporter (AAHS) family						
	BenK[b]	CAG68298.1	-	*Acinetobacter baylyi* ADP1	Benzoate	Collier *et al*. 1997
	BenK[b]	WP_011015098.1	-	*Corynebacterium glutamicum* ATCC 13032	Benzoate	Wang *et al*. 2011
	BenK[b]	WP_037061762.1	-	*Pseudomonas putida* CSV86	Benzoate	Choudhary *et al*. 2017
	BenP[b]	AAZ63295.1	-	*Cupriavidus pinatubonensis* JMP134	3-Chlorobenzoate	Ledger *et al*. 2009
	GalT[b]	CBJ94499.1	-	*Pseudomonas putida* KTGAL	Gallate	Nogales *et al*. 2011
	GenK[b]	WP_011015577.1	-	*Corynebacterium glutamicum* ATCC 13032	2,5-Dihydroxybenzoate	Xu *et al*. 2012b
	MhbT[b]	AAW63412.1	-	*Klebsiella pneumoniae* M5a1	3-Hydroxybenzoate	Xu *et al*. 2012a
	MhpT[b]	APC50650.1	-	*Escherichia coli* K-12 substr. W3110	3-(3-Hydroxyphenyl) propionate	Xu *et al*. 2013
	PcaK[b]	CAG68551.1	-	*Acinetobacter baylyi* ADP1	3,4-Dihydroxybenzoate, 4-Hydroxybenzoate, Vanillate	D'Argenio *et al*. 1999; Pernstich *et al*. 2014
	PcaK[b]	AAA85137.1	-	*Pseudomonas putida* PRS2000	3,4-Dihydroxybenzoate, 4-Hydroxybenzoate	Harwood *et al*. 1994;

					Nichols and Harwood 1997
TfdK[b]	AAZ65767.1	-	*Cupriavidus pinatubonensis* JMP134	2,4-Dichlorophenoxyacetate	Leveau *et al*. 1998
Metabolite:H^+ symporter (MHS) family					
CouT	ABG96912.1	-	*Rhodococcus jostii* RHA1	*p*-Coumarate, Ferulate	Otani *et al*. 2014
MopB	AAB41509.1	-	*Burkholderia cepacia* Pc701	4-Methyl-*o*-phthalate, Phthalate	Saint and Romas 1996
PhdT[c]	BAB97676.1	-	*Corynebacterium glutamicum* ATCC 13032	3-(4-Hydroxyphenyl)-3-propionate, *p*-Coumarate, Caffeate, Ferulate	Kallscheuer *et al*. 2016
Anion/cation symporter (ACS) family					
HpaX[b]	ADT77978.1	-	*Escherichia coli* W	4-Hydroxyphenylacetate	Prieto and García 1997
OphD[b]	BAG45577.1	-	*Burkholderia multivorans* ATCC 17616	Phthalate	Chang and Zylstra 1999
ATP-binding cassette (ABC)					
Hydrophobic amino acid uptake transporter (HAAT) family					
PcaM[c]	CAC49880.1	SBP	*Sinorhizobium meliloti* 1021	3,4-Dihydroxybenzoate	MacLean *et al*. 2011
PcaN[c]	CAC49879.1	TMD			
PcaV[c]	CAC49878.1	TMD			
PcaW[c]	CAC49877.1	NBD			

PcaX[c]	CAC49876.1	NBD			
HmgD[c]	AAY18216.1	SBP	*Pseudomonas putida* U	2,5-Dihydroxyphenylacetate	Arias-Barrau *et al*. 2005
HmgE[c]	AAY18215.1	TMD			
HmgF[c]	AAY18214.1	TMD			
HmgG[c]	AAY18213.1	NBD			
HmgH[c]	AAY18212.1	NBD			
Taurine uptake transporter (TauT) family					
OphF[b]	BAG45603.1	SBP	*Burkholderia multivorans* ATCC 17616	Phthalate	Chang *et al*. 2009
OphG	BAG45602.1	TMD			
OphH	BAG45601.1	NBD			
PatA	ABG99217.1	NBD	*Rhodococcus jostii* RHA1	Phthalate	Hara *et al*. 2010
PatB[b]	ABG99216.1	TMD			
PatC	ABG99215.1	TMD			
PatD	ABG99218.1	SBP			
Benzoate/H^+ symporter (BenE) family					
BenE1	AAN67649.1	-	*Pseudomonas putida* KT2440	Benzoate	Nishikawa *et al*. 2008
BenE2	AAN68775.1	-			
Divalent anion/Na^+ symporter (DASS) family					
GacP[c]	CCC80015.1	-	*Lactobacillus plantarum* WCFS1	Gallate	Reverón *et al*. 2017
Solute/sodium symporter (SSS) family					

PaaL[b]	AAC24338.1	-	*Pseudomonas putida* U	Phenylacetate	Olivera *et al*. 1998
Tripartite ATP-independent periplasmic transporter (TRAP-T) family					
FcbT1[b]	AAF16407.1	SBP	*Pseudomonas* sp. DJ-12	4-Chlorobenzoate	Chae and Zylstra 2006
FcbT2[b]	AAF16408.1	SC			
FcbT3[b]	AAF16409.1	LC			
TarP	CAE27223.1	SBP	*Rhodopseudomonas palustris* CGA009	*p*-Coumarate, Caffeate, Cinnamate, Ferulate	Salmon *et al*. 2013
TarQ	CAE27224.1	SC			
TarM	CAE27225.1	LC			
Tripartite tricarboxylate transporter (TTT) family					
TpiA[b]	BAN66716.1	LC	*Comamonas* sp. E6	Terephthalate	Hosaka *et al*. 2013
TpiB[b]	BAN66715.1	SC			
TphCII	BAE47084.1	SBP			

[a]LC, large component; NBD, nucleotide binding domain; SBP, substrate binding protein; SC, small component; TMD, transmembrane domain.

[b]The function of transporters has been experimentally verified by uptake assays with radioisotopes, biosensors or reconstituted proteoliposomes.

[c]The function of transporters has been experimentally examined by genetic disruption/complementation.

References (Table S4)

Arias-Barrau E, Sandoval A, Naharro G *et al*. A two-component hydroxylase involved in the assimilation of 3-hydroxyphenyl acetate in *Pseudomonas putida*. *J Biol Chem* 2005;280(28):26435-47.

Chae JC, Zylstra GJ. 4-chlorobenzoate uptake in *Comamonas* sp. strain DJ-12 is mediated by a tripartite ATP-independent periplasmic transporter. *J Bacteriol* 2006;188(24):8407-12.

Chang HK, Dennis JJ, Zylstra GJ. Involvement of two transport systems and a specific porin in the uptake of phthalate by *Burkholderia* spp. *J Bacteriol* 2009;191(14):4671-3.

Chang HK, Zylstra GJ. Characterization of the phthalate permease OphD from *Burkholderia cepacia* ATCC 17616. *J Bacteriol* 1999;181(19):6197-9.

Choudhary A, Purohit H, Phale PS. Benzoate transport in *Pseudomonas putida* CSV86. *FEMS Microbiol Lett* 2017;364(12).

Collier LS, Nichols NN, Neidle EL. *benK* encodes a hydrophobic permease-like protein involved in benzoate degradation by *Acinetobacter* sp. strain ADP1. *J Bacteriol* 1997;179(18):5943-6.

D'Argenio DA, Segura A, Coco WM *et al*. The physiological contribution of *Acinetobacter* PcaK, a transport system that acts upon protocatechuate, can be masked by the overlapping specificity of VanK. *J Bacteriol* 1999;181(11):3505-15.

Hara H, Stewart GR, Mohn WW. Involvement of a novel ABC transporter and monoalkyl phthalate ester hydrolase in phthalate ester catabolism by *Rhodococcus jostii* RHA1. *Appl Environ Microbiol* 2010;76(5):1516-23.

Harwood CS, Nichols NN, Kim MK *et al*. Identification of the *pcaRKF* gene cluster from *Pseudomonas putida*: involvement in chemotaxis, biodegradation, and transport of 4-hydroxybenzoate. *J Bacteriol* 1994;176(21):6479-88.

Hosaka M, Kamimura N, Toribami S *et al*. Novel tripartite aromatic acid transporter essential for terephthalate uptake in *Comamonas* sp. strain E6. *Appl Environ Microbiol* 2013;79(19):6148-55.

Kallscheuer N, Vogt M, Kappelmann J *et al*. Identification of the *phd* gene cluster responsible for phenylpropanoid utilization in *Corynebacterium glutamicum*. *Appl Microbiol Biotechnol* 2016;100(4):1871-81.

Ledger T, Aceituno F, Gonzalez B. 3-chlorobenzoate is taken up by a chromosomally encoded transport system in *Cupriavidus necator* JMP134. *Microbiology* 2009;155(Pt 8):2757-65.

Leveau JH, Zehnder AJ, van der Meer JR. The *tfdK* gene product facilitates uptake of 2,4-dichlorophenoxyacetate by *Ralstonia eutropha* JMP134(pJP4). *J Bacteriol* 1998;180(8):2237-43.

MacLean AM, Haerty W, Golding GB *et al*. The LysR-type PcaQ protein regulates expression of a protocatechuate-inducible ABC-type transport system in *Sinorhizobium meliloti*. *Microbiology* 2011;157(Pt 9):2522-33.

Nichols NN, Harwood CS. PcaK, a high-affinity permease for the aromatic compounds 4-hydroxybenzoate and protocatechuate from *Pseudomonas putida*. *J Bacteriol* 1997;179(16):5056-61.

Nishikawa Y, Yasumi Y, Noguchi S *et al*. Functional analyses of *Pseudomonas putida* benzoate transporters expressed in the yeast *Saccharomyces cerevisiae*. *Biosci Biotechnol Biochem*

2008;72(8):2034-8.

Nogales J, Canales A, Jiménez-Barbero J *et al*. Unravelling the gallic acid degradation pathway in bacteria: the *gal* cluster from *Pseudomonas putida*. *Mol Microbiol* 2011;79(2):359-74.

Olivera ER, Miñambres B, García B *et al*. Molecular characterization of the phenylacetic acid catabolic pathway in *Pseudomonas putida* U: the phenylacetyl-CoA catabolon. *Proc Natl Acad Sci USA* 1998;95(11):6419-24.

Otani H, Lee YE, Casabon I *et al*. Characterization of *p*-hydroxycinnamate catabolism in a soil Actinobacterium. *J Bacteriol* 2014;196(24):4293-303.

Pernstich C, Senior L, MacInnes KA *et al*. Expression, purification and reconstitution of the 4-hydroxybenzoate transporter PcaK from *Acinetobacter* sp. ADP1. *Protein Expr Purif* 2014;101(100):68-75.

Prieto MA, García JL. Identification of the 4-hydroxyphenylacetate transport gene of *Escherichia coli* W: construction of a highly sensitive cellular biosensor. *FEBS Lett* 1997;414(2):293-7.

Reverón I, Jiménez N, Curiel JA *et al*. Differential Gene Expression by *Lactobacillus plantarum* WCFS1 in Response to Phenolic Compounds Reveals New Genes Involved in Tannin Degradation. *Appl Environ Microbiol* 2017;83(7).

Saint CP, Romas P. 4-Methylphthalate catabolism in *Burkholderia* (*Pseudomonas*) *cepacia* Pc701: a gene encoding a phthalate-specific permease forms part of a novel gene cluster. *Microbiology* 1996;142 (Pt 9):2407-18.

Salmon RC, Cliff MJ, Rafferty JB *et al*. The CouPSTU and TarPQM transporters in *Rhodopseudomonas palustris*: redundant, promiscuous uptake systems for lignin-derived aromatic substrates. *PLoS One* 2013;8(3):e59844.

Wang SH, Xu Y, Liu SJ *et al*. Conserved residues in the aromatic acid/H^+ symporter family are important for benzoate uptake by NCgl2325 in *Corynebacterium glutamicum*. *Int Biodeterior Biodegradation* 2011;65(3):527-32.

Xu Y, Chen B, Chao H *et al*. *mhpT* encodes an active transporter involved in 3-(3-hydroxyphenyl)propionate catabolism by *Escherichia coli* K-12. *Appl Environ Microbiol* 2013;79(20):6362-8.

Xu Y, Gao X, Wang SH *et al*. MhbT is a specific transporter for 3-hydroxybenzoate uptake by Gram-negative bacteria. *Appl Environ Microbiol* 2012a;78(17):6113-20.

Xu Y, Wang SH, Chao HJ *et al*. Biochemical and molecular characterization of the gentisate transporter GenK in *Corynebacterium glutamicum*. *PLoS One* 2012b;7(7):e38701.

Table S5 Expression of genes encoding transporter except for MFS and ABC types

Family	Replicon	Locus	Component[a]	Protein	Accession number	%Amino acid identity	3-CB vs. CA		BA vs. CA		3-CB vs. BA	
							LogFC[b]	FDR	LogFC[c]	FDR	LogFC[d]	FDR
Benzoate/H^+ symporter (BenE) family												
	Chr.1	BJN34_14300	-	BenE2	AAN68775.1	47.1	-0.26	4.8E-01	-0.26	6.0E-01	0.00093	1.0E+00
Divalent anion/Na^+ symporter (DASS) family												
	Chr.1	BJN34_03715	-	GacP	CCC80015.1	20.9	-1.4	7.1E-04	-0.15	8.5E-01	-1.2	8.9E-03
Solute/sodium symporter (SSS) family												
	Chr.1	BJN34_08680	-	PaaL	AAC24338.1	65.1	3.1	1.5E-15	3.2	3.0E-16	-0.11	8.9E-01
		BJN34_13555	-			32.6	0.32	4.0E-01	0.32	5.2E-01	-0.0016	1.0E+00
	Chr.2	BJN34_22225	-	PaaL	AAC24338.1	60.4	1.4	4.8E-02	1.8	2.0E-02	-0.35	7.2E-01
		BJN34_26835	-			24.1	2.6	9.5E-04	2.4	7.0E-03	0.26	8.6E-01
		BJN34_29130	-			64.3	-1.3	2.1E-01	-2.2	6.1E-02	0.87	5.8E-01
		BJN34_32040	-			77.9	-1.9	6.2E-02	0.37	8.2E-01	-2.3	4.8E-02
Tripartite ATP-independent periplasmic transporter (TRAP-T) family												
	Chr.1	BJN34_06770	SC	TarQ	CAE27224.1	16.7	-0.20	6.7E-01	0.27	6.5E-01	-0.47	3.6E-01
		BJN34_06775	LC	TarM	CAE27225.1	29.3	-0.30	4.0E-01	-0.23	6.6E-01	-0.075	9.0E-01
		BJN34_06780	SBP	TarP	CAE27223.1	23.0	-0.74	1.6E-02	-0.44	2.7E-01	-0.30	5.2E-01
	Chr.2	BJN34_30790	SBP	FcbT1	AAF16407.1	22.3	-0.59	1.8E-01	-0.63	2.3E-01	0.040	9.6E-01
		BJN34_30795	SC	FcbT2	AAF16408.1	17.1	-0.73	3.8E-01	-1.2	2.3E-01	0.44	7.3E-01
		BJN34_30800	LC	FcbT3	AAF16409.1	30.9	-1.5	4.4E-03	-0.62	4.1E-01	-0.92	2.0E-01
Tripartite tricarboxylate transporter (TTT) family												
	Chr.1	BJN34_14920	SBP	TphCII	BAE47084.1	33.9	-0.30	3.2E-01	-0.27	5.2E-01	-0.038	9.5E-01
		BJN34_14930	SC	TpiB	BAN66715.1	41.0	0.69	3.2E-01	2.5	6.5E-05	-1.8	6.4E-03
		BJN34_14935	LC	TpiA	BAN66716.1	76.1	0.45	4.6E-01	1.8	7.6E-04	-1.4	1.9E-02
		BJN34_19840	SBP	TphCII	BAE47084.1	25.2	-4.2	3.8E-10	-4.8	3.2E-12	0.62	5.4E-01

BJN34_19845	SC	TpiB	BAN66715.1	21.1	-4.7	9.4E-12	-4.6	2.8E-11	-0.071	9.6E-01
BJN34_19850	LC	TpiA	BAN66716.1	46.1	-4.6	8.3E-16	-4.6	1.3E-15	0.0061	1.0E+00

[a]LC, large component; SBP, substrate binding protein; SC, small component.

[b]Log fold-change values calculated from 3-CB/CA.

[c]Log fold-change values calculated from BA/CA.

[d]Log fold-change values calculated from 3-CB/BA.

Table S6 Summury of enriched GO terms

Analysis condition	Category[a]	GO term	GO ID	Number of sequences	Log fold-change[b]	Z score	P-value	FDR
3-Chlorobenzoate vs. Citric acid	MF	structural constituent of ribosome	GO:0003735	44	-2.6	-12.3	0	0
	CC	ribosome	GO:0005840	42	-2.6	-12.0	0	0
	BP	translation	GO:0006412	43	-2.6	-12.1	0	0
	BP	cellular aromatic compound metabolic process	GO:0006725	23	2.6	7.9	2.4E-15	7.0E-14
	BP	oxidation-reduction process	GO:0055114	608	0.60	7.1	1.1E-12	2.4E-11
	MF	oxidoreductase activity	GO:0016491	328	0.75	7.0	1.9E-12	3.7E-11
	MF	iron ion binding	GO:0005506	35	1.7	6.2	7.2E-10	1.2E-08
	MF	catalytic activity	GO:0003824	342	0.63	5.7	1.1E-08	1.6E-07
	MF	RNA binding	GO:0003723	47	-1.1	-5.6	2.0E-08	2.5E-07
	MF	2 iron, 2 sulfur cluster binding	GO:0051537	26	1.8	5.5	4.2E-08	4.9E-07
	MF	ferric iron binding	GO:0008199	17	1.9	4.9	9.6E-07	1.0E-05
	MF	nucleic acid binding	GO:0003676	48	-0.81	-4.6	4.9E-06	4.7E-05
	MF	CoA-transferase activity	GO:0008410	52	1.0	4.0	7.1E-05	6.3E-04
	MF	metal ion binding	GO:0046872	49	0.94	3.6	3.3E-04	2.7E-03
	MF	aminoacyl-tRNA ligase activity	GO:0004812	19	-1.0	-3.5	4.0E-04	3.1E-03
	MF	GTP binding	GO:0005525	26	-0.80	-3.3	9.1E-04	6.5E-03
	BP	tRNA aminoacylation for protein translation	GO:0006418	14	-1.1	-3.3	1.0E-03	7.1E-03
	MF	endonuclease activity	GO:0004519	11	-1.2	-3.1	1.7E-03	1.1E-02
	MF	ATPase activity	GO:0016887	136	0.54	2.9	3.8E-03	2.3E-02
	MF	peptidyl-prolyl cis-trans isomerase activity	GO:0003755	11	-1.1	-2.8	4.6E-03	2.7E-02
	MF	nucleotide binding	GO:0000166	35	-0.52	-2.8	5.8E-03	3.2E-02
	MF	iron-sulfur cluster binding	GO:0051536	57	0.70	2.7	7.1E-03	3.7E-02

	MF	structural constituent of ribosome	GO:0003735	44	-1.4	-9.9	0	0
	CC	ribosome	GO:0005840	42	-1.4	-9.7	0	0
	BP	translation	GO:0006412	43	-1.4	-9.9	0	0
	BP	bacterial-type flagellum-dependent cell motility	GO:0071973	14	2.0	6.9	6.4E-12	1.8E-10
	BP	cellular aromatic compound metabolic process	GO:0006725	23	1.3	5.5	3.3E-08	7.6E-07
	MF	oxidoreductase activity	GO:0016491	328	0.42	5.0	5.0E-07	9.7E-06
	MF	catalytic activity	GO:0003824	342	0.40	4.9	1.2E-06	1.9E-05
	MF	RNA binding	GO:0003723	47	-0.57	-4.6	4.5E-06	6.0E-05
	MF	CoA-transferase activity	GO:0008410	52	0.79	4.6	4.7E-06	6.0E-05
	MF	iron ion binding	GO:0005506	35	0.89	4.3	1.5E-05	1.7E-04
Benzoate	MF	nucleic acid binding	GO:0003676	48	-0.50	-4.2	3.2E-05	3.3E-04
vs.	BP	oxidation-reduction process	GO:0055114	608	0.30	3.9	8.2E-05	7.9E-04
Citric acid	MF	endonuclease activity	GO:0004519	11	-1.0	-3.5	4.4E-04	3.9E-03
	MF	ATPase activity	GO:0016887	136	0.42	3.2	1.3E-03	1.1E-02
	MF	GTP binding	GO:0005525	26	-0.49	-3.0	2.4E-03	1.9E-02
	MF	porin activity	GO:0015288	53	-0.30	-3.0	2.6E-03	1.9E-02
	MF	oxidoreductase activity, acting on the CH-OH group of donors, NAD or NADP as acceptor	GO:0016616	26	-0.47	-3.0	3.1E-03	2.1E-02
	BP	tRNA aminoacylation for protein translation	GO:0006418	14	-0.69	-2.9	3.2E-03	2.1E-02
	MF	aminoacyl-tRNA ligase activity	GO:0004812	19	-0.55	-2.8	4.4E-03	2.7E-02
	MF	iron-sulfur cluster binding	GO:0051536	57	0.51	2.8	5.6E-03	3.2E-02
	BP	peptide transport	GO:0015833	11	1.0	2.7	7.8E-03	4.2E-02
	MF	GTPase activity	GO:0003924	12	-0.67	-2.7	8.0E-03	4.2E-02
3-Chlorobenzoate	MF	structural constituent of ribosome	GO:0003735	44	-1.2	-7.4	1.5E-13	1.2E-11
vs.	CC	ribosome	GO:0005840	42	-1.2	-7.3	3.1E-13	1.2E-11
Benzoate	BP	translation	GO:0006412	43	-1.2	-7.3	3.2E-13	1.2E-11

BP	bacterial-type flagellum-dependent cell motility	GO:0071973	14	-1.8	-6.4	1.2E-10	3.3E-09
BP	oxidation-reduction process	GO:0055114	608	0.31	6.1	1.3E-09	2.9E-08
BP	cellular aromatic compound metabolic process	GO:0006725	23	1.3	5.6	1.7E-08	3.3E-07
MF	2 iron, 2 sulfur cluster binding	GO:0051537	26	1.1	5.2	2.3E-07	3.8E-06
BP	signal transduction	GO:0007165	72	-0.61	-5.1	2.6E-07	3.8E-06
BP	chemotaxis	GO:0006935	16	-1.3	-5.0	5.4E-07	7.0E-06
MF	oxidoreductase activity	GO:0016491	328	0.33	4.9	9.4E-07	1.1E-05
MF	ferric iron binding	GO:0008199	17	1.3	4.8	1.9E-06	2.0E-05
MF	iron ion binding	GO:0005506	35	0.84	4.4	1.3E-05	1.3E-04
MF	metal ion binding	GO:0046872	49	0.56	3.4	7.8E-04	6.7E-03
MF	RNA binding	GO:0003723	47	-0.48	-3.3	8.1E-04	6.7E-03
MF	catalytic activity	GO:0003824	342	0.23	3.2	1.3E-03	9.9E-03

[a]BP, Biological Process; CC, Cellular Component; MF, Molecular Function.

[b]Log fold-change values in 3-Chlorobenzoate vs. Citric acid, Benzoate vs. Citric acid, and 3-Chlorobenzoate vs. Benzoate were calculated from 3-CB/CA, BA/CA, and 3-CB/BA, respectively.

Table S7 Detailed information of genes classified as GO:0006935, GO:0007165, and GO:0071973 terms

Replicon	Locus	Gene	K number	KEGG definition	3-CB vs. CA		BA vs. CA		3-CB vs. BA	
					LogFC[a]	FDR	LogFC[b]	FDR	LogFC[c]	FDR
bacterial-type flagellum-dependent cell motility (GO:0071973)										
Chr.2	BJN34_22000	*flgB*	K02387	flagellar basal-body rod protein FlgB	1.5	1.0E-01	2.3	2.1E-02	-0.80	5.5E-01
	BJN34_22005	*flgC*	K02388	flagellar basal-body rod protein FlgC	1.7	4.7E-02	2.5	5.8E-03	-0.84	4.9E-01
	BJN34_22015	*flgE*	K02390	flagellar hook protein FlgE	0.77	4.3E-01	2.0	4.4E-02	-1.2	2.8E-01
	BJN34_22020	*flgF*	K02391	flagellar basal-body rod protein FlgF	0.65	5.2E-01	2.1	3.6E-02	-1.5	1.9E-01
	BJN34_22025	*flgG*	K02392	flagellar basal-body rod protein FlgG	0.71	4.7E-01	2.2	2.2E-02	-1.5	1.7E-01
	BJN34_22030	*flgH*	K02393	flagellar L-ring protein precursor FlgH	0.54	5.7E-01	2.3	1.2E-02	-1.8	7.7E-02
	BJN34_22035	*flgI*	K02394	flagellar P-ring protein precursor FlgI	0.57	5.8E-01	2.4	1.6E-02	-1.8	8.9E-02
	BJN34_22045	*flgK*	K02396	flagellar hook-associated protein 1 FlgK	-1.7	3.0E-02	1.7	5.7E-02	-3.4	3.2E-05
	BJN34_22050	*flgL*	K02397	flagellar hook-associated protein 3 FlgL	-1.4	8.8E-02	2.3	9.6E-03	-3.7	1.3E-05
	BJN34_24450	*fliM*	K02416	flagellar motor switch protein FliM	0.55	4.5E-01	1.8	8.6E-03	-1.3	1.0E-01
	BJN34_24455	*fliL*	K02417	flagellar FliL protein	0.61	3.9E-01	1.8	8.8E-03	-1.2	1.2E-01
	BJN34_34110	*fliC*	K02406	flagellin	-2.6	4.4E-05	1.1	1.6E-01	-3.7	1.9E-08
	BJN34_34145	*fliE*	K02408	flagellar hook-basal body complex protein FliE	1.2	1.5E-01	2.3	6.8E-03	-1.1	2.8E-01
	BJN34_34170	*fliJ*	K02413	flagellar FliJ protein	0.17	8.8E-01	1.7	9.3E-02	-1.5	1.6E-01
chemotaxis (GO:0006935)										
Chr.1	BJN34_04180	*pilI*	K02659	twitching motility protein PilI	0.80	9.4E-03	0.43	3.0E-01	0.36	4.0E-01
	BJN34_04190	*chpA*	K06596	chemosensory pili system protein ChpA	0.062	8.8E-01	0.24	6.1E-01	-0.17	7.2E-01
	BJN34_11685	*tsr*	K05874	methyl-accepting chemotaxis protein I, serine sensor receptor	-0.75	9.4E-02	0.60	2.7E-01	-1.3	3.0E-03
Chr.2	BJN34_21800	*tsr*	K05874	methyl-accepting chemotaxis protein I, serine sensor receptor	-2.3	2.6E-06	1.6	2.6E-03	-3.9	7.0E-15
	BJN34_21835	*cheW*	K03408	purine-binding chemotaxis protein CheW	-2.6	1.2E-03	1.3	1.9E-01	-3.9	4.0E-06

	BJN34_21875	*cheA*	K03407	two-component system, chemotaxis family, sensor kinase CheA	-1.2	1.4E-03	1.5	1.8E-04	-2.7	4.1E-13
	BJN34_21880	*cheW*	K03408	purine-binding chemotaxis protein CheW	-1.1	1.3E-02	1.6	8.4E-04	-2.7	1.0E-09
	BJN34_21890	*cheD*	K03411	chemotaxis protein CheD	-0.63	7.6E-02	1.6	1.1E-06	-2.2	2.0E-12
	BJN34_21895	*cheB*	K03412	two-component system, chemotaxis family, protein-glutamate methylesterase/glutaminase	-0.84	5.7E-03	1.4	1.6E-06	-2.3	2.0E-15
	BJN34_24455	*fliL*	K02415	flagellar FliL protein	0.61	3.9E-01	1.8	8.8E-03	-1.2	1.2E-01
	BJN34_27975	-	K02484	two-component system, OmpR family, sensor kinase	0.16	6.2E-01	0.00058	1.0E+00	0.16	7.2E-01
	BJN34_32590	*wspB*	K13488	chemotaxis-related protein WspB	0.63	3.3E-01	-0.36	7.2E-01	0.99	1.8E-01
	BJN34_32600	*wspD*	K13489	chemotaxis-related protein WspD	-0.12	8.6E-01	-0.63	3.7E-01	0.51	5.0E-01
	BJN34_32605	*wspE*	K13490	two-component system, chemotaxis family, sensor histidine kinase and response regulator WspE	-0.041	9.3E-01	-0.49	3.2E-01	0.45	3.8E-01
	BJN34_32610	*wspF*	K13491	two-component system, chemotaxis family, response regulator WspF	-0.084	8.3E-01	-0.50	1.8E-01	0.41	3.0E-01
	BJN34_33670	*cheV*	K03415	two-component system, chemotaxis family, chemotaxis protein CheV	-1.7	2.4E-03	1.7	7.4E-03	-3.4	3.9E-09
signal transduction (GO:0007165)										
	BJN34_00285	*mcp*	K03406	methyl-accepting chemotaxis protein	-2.7	1.3E-06	0.11	9.2E-01	-2.8	8.7E-07
	BJN34_01755	*creC*	K07641	two-component system, OmpR family, sensor histidine kinase CreC	-0.25	4.6E-01	0.18	7.1E-01	-0.44	2.6E-01
Chr.1	BJN34_01935	-	K02484	two-component system, OmpR family, sensor kinase	0.0086	9.9E-01	0.17	7.8E-01	-0.16	7.9E-01
	BJN34_03290	*tctE*	K07649	two-component system, OmpR family, sensor histidine kinase TctE	0.65	2.8E-02	0.21	6.6E-01	0.43	2.6E-01
	BJN34_03520	*envZ*	K07638	two-component system, OmpR family,	0.13	7.6E-01	-0.12	8.6E-01	0.25	6.3E-01

			osmolarity sensor histidine kinase EnvZ						
BJN34_04180	*pilI*	K02659	twitching motility protein PilI	0.80	9.4E-03	0.43	3.0E-01	0.36	4.0E-01
BJN34_04185	*pilJ*	K02660	twitching motility protein PilJ	-0.094	8.6E-01	0.11	8.9E-01	-0.20	7.6E-01
BJN34_04190	*chpA*	K06596	chemosensory pili system protein ChpA	0.062	8.8E-01	0.24	6.1E-01	-0.17	7.2E-01
BJN34_07255	*qseC*	K07645	two-component system, OmpR family, sensor histidine kinase QseC	0.010	9.8E-01	0.08	8.9E-01	-0.071	9.0E-01
BJN34_07405	*envZ*	K07638	two-component system, OmpR family, osmolarity sensor histidine kinase EnvZ	-0.51	7.9E-02	0.17	7.3E-01	-0.68	3.7E-02
BJN34_08650	-	-	chemotaxis protein[d]	-1.9	5.0E-03	-1.9	1.1E-02	-0.00035	1.0E+00
BJN34_09575	*tsr*	K05874	methyl-accepting chemotaxis protein I, serine sensor receptor	-4.4	2.3E-23	1.3	6.2E-03	-5.6	9.9E-35
BJN34_11685	*tsr*	K05874	methyl-accepting chemotaxis protein I, serine sensor receptor	-0.75	9.4E-02	0.60	2.7E-01	-1.3	3.0E-03
BJN34_11890	*glnL*	K07708	two-component system, NtrC family, nitrogen regulation sensor histidine kinase GlnL	-0.058	9.0E-01	-0.64	1.3E-01	0.58	1.9E-01
BJN34_12140	*tctE*	K07649	two-component system, OmpR family, sensor histidine kinase TctE	-0.066	9.3E-01	0.02	9.8E-01	-0.090	9.3E-01
BJN34_13080	*phoR*	K07636	two-component system, OmpR family, phosphate regulon sensor histidine kinase PhoR	0.15	6.6E-01	-0.03	9.6E-01	0.18	6.9E-01
BJN34_13375	-	-	hybrid sensor histidine kinase/response regulator[d]	3.0	6.4E-03	2.5	4.7E-02	0.46	7.9E-01
BJN34_13395	-	-	sensor domain-containing diguanylate cyclase[d]	1.0	5.6E-03	0.88	4.7E-02	0.17	8.0E-01
BJN34_13925	*kdpD*	K07646	two-component system, OmpR family, sensor histidine kinase KdpD	0.14	6.7E-01	0.11	8.3E-01	0.032	9.5E-01
BJN34_16260	-	-	hybrid sensor histidine kinase/response regulator[d]	0.32	4.0E-01	-0.13	8.4E-01	0.45	3.3E-01
BJN34_16640	*phcR*	K19622	two-component system, response regulator PhcR	0.53	8.7E-02	0.56	1.2E-01	-0.030	9.6E-01
BJN34_16645	*phcS*	K19621	two-component system,	0.21	5.1E-01	0.18	7.1E-01	0.036	9.5E-01

				sensor histidine kinase PhcS						
	BJN34_17005	*mcp*	K03406	methyl-accepting chemotaxis protein	-0.019	9.9E-01	0.016	9.9E-01	-0.035	9.8E-01
	BJN34_17200	*pilS*	K02668	two-component system, NtrC family, sensor histidine kinase PilS	-0.10	7.8E-01	-0.026	9.7E-01	-0.070	8.9E-01
	BJN34_18130	-	K02484	two-component system, OmpR family, sensor kinase	0.77	8.3E-02	0.39	5.6E-01	0.38	5.6E-01
	BJN34_19640	-	-	histidine kinase[d]	1.1	1.7E-04	0.42	2.8E-01	0.64	6.6E-02
	BJN34_19710	-	-	PAS domain-containing sensor histidine kinase[d]	-0.42	1.4E-01	-0.062	9.0E-01	-0.36	3.3E-01
	BJN34_19875	*tctE*	K07649	two-component system, OmpR family, sensor histidine kinase TctE	-0.57	6.8E-02	0.23	6.2E-01	-0.80	1.6E-02
Chr.2	BJN34_21375	*mcp*	K03406	methyl-accepting chemotaxis protein	-0.86	2.4E-02	-0.10	8.9E-01	-0.76	1.0E-01
	BJN34_21525	-	K02482	two-component system, NtrC family, sensor kinase	0.27	8.0E-01	0.18	9.1E-01	0.086	9.6E-01
	BJN34_21800	*tsr*	K05874	methyl-accepting chemotaxis protein I, serine sensor receptor	-2.3	2.6E-06	1.6	2.6E-03	-3.9	7.0E-15
	BJN34_21835	*cheW*	K03408	purine-binding chemotaxis protein CheW	-2.6	1.2E-03	1.3	1.9E-01	-3.9	4.0E-06
	BJN34_21840	*aer*	K03776	aerotaxis receptor	-2.8	1.7E-05	1.4	7.4E-02	-4.2	8.0E-10
	BJN34_21845	*mcp*	K03406	methyl-accepting chemotaxis protein	-2.9	9.7E-06	1.4	7.8E-02	-4.3	4.3E-10
	BJN34_21875	*cheA*	K03407	two-component system, chemotaxis family, sensor kinase CheA	-1.2	1.4E-03	1.5	1.8E-04	-2.7	4.1E-13
	BJN34_21880	*cheW*	K03408	purine-binding chemotaxis protein CheW	-1.1	1.3E-02	1.6	8.4E-04	-2.7	1.0E-09
	BJN34_22870	-	-	two-component sensor histidine kinase[d]	1.1	3.2E-03	0.27	6.7E-01	0.80	6.7E-02
	BJN34_23155	*kdpD*	K07646	two-component system, OmpR family, sensor histidine kinase KdpD	-0.24	8.6E-01	-0.53	7.7E-01	0.29	8.8E-01
	BJN34_23640	-	-	two-component sensor histidine kinase[d]	0.57	6.2E-02	0.10	8.6E-01	0.46	2.2E-01

BJN34_23675	*mcp*	K03406	methyl-accepting chemotaxis protein	-1.8	1.4E-04	1.0	8.1E-02	-2.8	5.1E-09
BJN34_23945	-	-	two-component sensor histidine kinase[d]	0.16	6.9E-01	0.12	8.4E-01	0.038	9.5E-01
BJN34_24020	*cqsS*	K10916	two-component system, CAI-1 autoinducer sensor kinase/phosphatase CqsS	-0.078	8.5E-01	-0.29	5.2E-01	0.21	6.6E-01
BJN34_24350	*tsr*	K05874	methyl-accepting chemotaxis protein I, serine sensor receptor	4.2	1.3E-43	4.6	2.9E-49	-0.36	4.2E-01
BJN34_25245	*aer*	K03776	aerotaxis receptor	-1.6	1.6E-04	1.8	1.6E-05	-3.4	1.9E-16
BJN34_26260	*rcsC*	K07677	two-component system, NarL family, capsular synthesis sensor histidine kinase RcsC	-0.46	2.7E-01	-0.48	3.6E-01	0.017	9.9E-01
BJN34_27085	*evgS*	K07679	two-component system, NarL family, sensor histidine kinase EvgS	0.56	4.4E-01	0.27	8.2E-01	0.30	7.8E-01
BJN34_27885	-	-	chemotaxis protein[d]	-0.39	7.4E-01	-1.3	3.0E-01	0.94	5.2E-01
BJN34_27975	-	K02484	two-component system, OmpR family, sensor kinase	0.16	6.2E-01	0.00058	1.0E+00	0.16	7.2E-01
BJN34_28775	*cusS*	K07644	two-component system, OmpR family, heavy metal sensor histidine kinase CusS	0.91	6.3E-02	0.85	1.5E-01	0.062	9.5E-01
BJN34_28820	-	-	sensor histidine kinase[d]	0.61	1.5E-01	0.50	3.6E-01	0.11	8.8E-01
BJN34_29045	-	-	PAS domain S-box protein[d]	0.77	3.6E-03	0.50	1.2E-01	0.27	5.2E-01
BJN34_29565	-	-	hybrid sensor histidine kinase/response regulator[d]	1.4	3.3E-04	0.49	3.8E-01	0.88	6.0E-02
BJN34_29890	*cusS*	K07644	two-component system, OmpR family, heavy metal sensor histidine kinase CusS	0.71	6.8E-02	0.45	4.1E-01	0.26	6.6E-01
BJN34_31545	-	K02482	two-component system, NtrC family, sensor kinase	1.3	4.5E-03	0.84	1.6E-01	0.50	4.7E-01
BJN34_31830	*tctE*	K07649	two-component system, OmpR family, sensor histidine kinase TctE	-1.7	1.1E-04	-2.5	6.7E-08	0.77	2.3E-01
BJN34_32190	*mcp*	K03406	methyl-accepting chemotaxis protein	-1.8	4.7E-05	1.5	2.7E-03	-3.3	3.0E-13

	BJN34_32420	*rcsC*	K07677	two-component system, NarL family, capsular synthesis sensor histidine kinase RcsC	0.048	9.5E-01	0.78	2.1E-01	-0.73	2.6E-01
	BJN34_32585	*wspA*	K13487	methyl-accepting chemotaxis protein WspA	0.20	5.8E-01	-0.36	4.1E-01	0.56	1.5E-01
	BJN34_32590	*wspB*	K13488	chemotaxis-related protein WspB	0.63	3.3E-01	-0.36	7.2E-01	0.99	1.8E-01
	BJN34_32600	*wspD*	K13489	chemotaxis-related protein WspD	-0.12	8.6E-01	-0.63	3.7E-01	0.51	5.0E-01
	BJN34_32605	*wspE*	K13490	two-component system, chemotaxis family, sensor histidine kinase and response regulator WspE	-0.041	9.3E-01	-0.49	3.2E-01	0.45	3.8E-01
	BJN34_33085	*rcsC*	K07677	two-component system, NarL family, capsular synthesis sensor histidine kinase RcsC	-0.81	4.1E-01	0.034	9.8E-01	-0.84	5.1E-01
	BJN34_33100	*rcsC*	K07677	two-component system, NarL family, capsular synthesis sensor histidine kinase RcsC	0.26	4.6E-01	0.25	6.0E-01	0.0057	9.9E-01
	BJN34_33185	*tsr*	K05874	methyl-accepting chemotaxis protein I, serine sensor receptor	-2.8	7.8E-08	0.84	2.1E-01	-3.7	7.7E-12
	BJN34_33425	*cusS*	K07644	two-component system, OmpR family, heavy metal sensor histidine kinase CusS	0.32	4.2E-01	0.18	7.8E-01	0.14	8.2E-01
	BJN34_33670	*cheV*	K03415	two-component system, chemotaxis family, chemotaxis protein CheV	-1.7	2.4E-03	1.7	7.4E-03	-3.4	3.9E-09
	BJN34_33995	*narX*	K07673	two-component system, NarL family, nitrate/nitrite sensor histidine kinase NarX	-0.37	4.4E-01	-0.18	8.2E-01	-0.19	7.9E-01
	BJN34_34065	-	-	hybrid sensor histidine kinase/response regulator[d]	0.38	3.1E-01	-0.0015	1.0E+00	0.38	4.3E-01
	BJN34_34080	-	-	hybrid sensor histidine kinase/response regulator[d]	0.60	5.5E-01	0.19	9.1E-01	0.41	7.8E-01
	BJN34_34800	*mcp*	K03406	methyl-accepting chemotaxis protein	-3.0	9.6E-09	0.72	2.9E-01	-3.7	2.0E-12
	BJN34_35100	-	K02484	two-component system, OmpR family, sensor kinase	0.060	9.8E-01	1.0	6.9E-01	-0.99	7.1E-01
pENH92	BJN34_36140	-	-	hybrid sensor histidine kinase/response regulator[d]	1.5	1.4E-04	0.37	5.6E-01	1.1	1.4E-02

[a]Log fold-change values calculated from 3-CB/CA.

[b]Log fold-change values calculated from BA/CA.

[c]Log fold-change values calculated from 3-CB/BA.

[d]Annotation from GenBank.

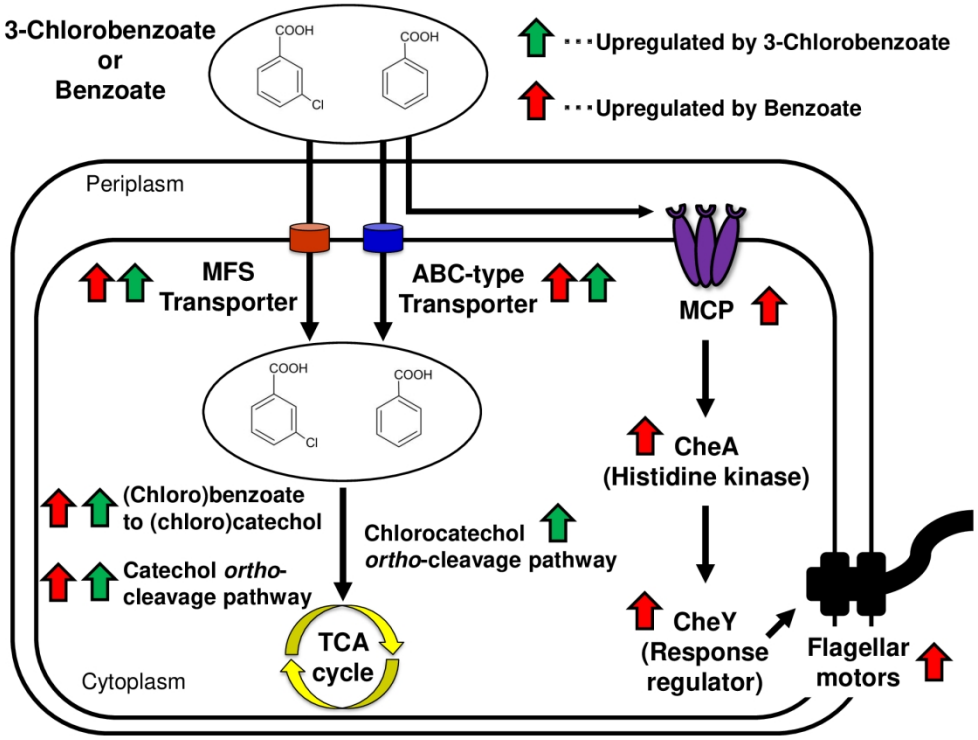

RNA-seq analysis showed that 3-chlorobenzoate and benzoate induced the expression of genes for aromatic degradation, transport, and/or chemotaxis strongly in *Cupriavidus necator* NH9.

254x190mm (200 x 200 DPI)